



Zoological Journal of the Linnean Society, 2012, 164, 669–713. With 37 figures

# Craniodental characters and the relationships of Procyonidae (Mammalia: Carnivora)

HEATHER E. AHRENS\*†

Jackson School of Geosciences, University of Texas at Austin, 1 University Station C1100, Austin, TX 78712, USA

Received 5 August 2011; accepted for publication 6 August 2011

Recent phylogenies of Procyonidae based on molecular data differ significantly from previous morphology-based phylogenies in all generic sister taxon relationships. I have compiled the most comprehensive dataset of craniodental morphology that incorporates previous morphological characters, and with the aid of high-resolution X-ray computed tomography, new characters. This expanded craniodental analysis is based on 78 characters and yields new phylogenetic results regarding the ingroup relationships of Procyonidae. These results include *Bassariscus astutus* as the least derived member of Procyonidae and *Ailurus fulgens* nested well within the clade. Additionally, there are some similarities to previous morphological analyses of Procyonidae. Although the characters used to unite and diagnose Procyonidae vary depending on the phylogenetic analysis and have ambiguous taxonomic distribution amongst both Procyonidae and Musteloidea, there is significant morphological support for clades within Procyonidae. In addition to the strength of the morphological support within the clade, the disparate topographical regions of the skull from which the characters are derived may indicate that these synapomorphies are indeed the result of homology rather than adaptive convergence, as suggested by analyses based on molecular data.

© 2012 The Linnean Society of London, *Zoological Journal of the Linnean Society*, 2012, 164, 669–713.  
doi: 10.1111/j.1096-3642.2011.00778.x

ADDITIONAL KEYWORDS: adaptive convergence – *Ailurus fulgens* – fossil procyonids – morphology – phylogeny.

## INTRODUCTION

Procyonidae is a relatively small mammalian family, yet includes species that exhibit a wide range of feeding ecologies and craniodental morphologies. Crown group Procyonidae includes the genera *Procyon*, *Nasua*, *Nasuella*, *Bassariscus*, *Bassaricyon*, and *Potos* (Wozencraft, 2005). The clade has been intensively studied in the biological literature with regard to population size (Gehrt, 2003; Prange, Gehrt & Wiggers, 2003), sexual dimorphism (Kennedy & Lindsay, 1984; Ritke, 1990), and geographical

variation (Goldman, 1950; Wright & Lundelius, 1963). Historical classification schemes of the family are also numerous (Turner, 1848; Flower, 1869; Gray, 1869; Gill, 1874; Mivart, 1885; Hollister, 1915; Pocock, 1921). However, those classifications differed on which taxa belong in Procyonidae and the relationships of members within the clade. Controversy particularly surrounded placement of *Bassariscus*, *Potos*, *Bassaricyon*, and *Ailurus fulgens*, the red panda. Here, I recover a monophyletic Procyonidae that consists of the most recent common ancestor of *Bassariscus astutus*, *Potos flavus*, and *Procyon lotor* and all of that ancestor's descendants.

Since the development of phylogenetic systematics, relationships within Procyonidae have been re-evaluated for both extant and extinct members of the group. The monophyly of Procyonidae, excluding the

\*E-mail: hahrens1@jhmi.edu

†Current address: Center for Functional Anatomy and Evolution, Johns Hopkins University School of Medicine, 1830 E. Monument St., Room 308, Baltimore, MD 21205, USA.

red panda, is generally unquestioned (Decker & Wozencraft, 1991; Wyss & Flynn, 1993; Finarelli, 2008; Eizirik *et al.*, 2010), although one recent carnivoran phylogeny based on molecular data recovered a polyphyletic Procyonidae (Agnarsson, Kuntner & May-Colado, 2010), with *Potos flavus* as sister to all other musteloids. The ingroup relationships are largely incongruent between the morphological and molecular analyses (Decker & Wozencraft, 1991; Baskin, 2004; Fulton & Strobeck, 2007; Koepfli *et al.*, 2007; Wolsan & Sato, 2010). Additional controversy surrounds the phylogenetic affinities of *Ailurus fulgens* and the relationships within Musteloidea, which includes *Ailurus fulgens*, mephitids, mustelids, and procyonids (Wyss & Flynn, 1993; Dragoo & Honeycutt, 1997; Wang, 1997; Bininda-Emonds, Gittleman & Purvis, 1999; Flynn *et al.*, 2000, 2005). The unresolved relationships within Musteloidea probably contribute to the conflict between morphological and molecular analyses of Procyonidae because of conflicting outgroup polarization, as well as disparate taxon sampling.

Several morphological analyses of evolutionary relationships within Procyonidae have previously been published (Baskin, 1982, 1989, 2004; Decker & Wozencraft, 1991), with the two most recent studies providing the most thorough analyses. The generic relationships of extant members of Procyonidae were the focus of Decker & Wozencraft's (1991) study. That dataset included 37 cranial characters, 14 dental characters, seven postcranial characters, and six soft tissue characters. Parsimony analysis of those data recovered a monophyletic Procyonidae with *Bassaricyon* and *Potos* as sister taxa in Potosinae, and *Bassariscus*, *Procyon*, *Nasuella*, and *Nasua* as a clade, Procyoninae (Fig. 1A). A subsequent phylogenetic analysis of the generic relationships of both extant and extinct New World procyonids was based on ten cranial and 30 dental characters (Baskin, 2004). Parsimony analysis of those data yielded a monophyletic New World Procyoninae, comprised of two sister taxa: Potosini and Procyonini (Fig. 1B). The phylogenies recovered by the two analyses are congruent with one another with respect to the extant members.

Two molecular phylogenetic analyses focusing on the relationships of extant procyonids were based on 11 nuclear and four mitochondrial gene sequences (Fulton & Strobeck, 2007; Koepfli *et al.*, 2007). The resulting tree consisted of *Potos flavus* as the sister taxon to all remaining members of Procyonidae, with a clade composed of *Bassaricyon* plus *Nasua* sister to a clade composed of *Procyon* plus *Bassariscus* (Fig. 1C–D). Additionally, a combined analysis of molecular and morphological data was performed using Baskin's (2004) morphological dataset (Koepfli *et al.*, 2007). Unfortunately, the morphological characters incorporated in that analysis were almost entirely dental and

did not include the numerous cranial characters provided by Decker & Wozencraft (1991).

Most morphological studies (Baskin, 1982, 1989, 2004) relied heavily on dental characters even though the wide range of feeding ecologies in procyonids may lead to adaptive convergences that could confound phylogenetic analyses (Koepfli *et al.*, 2007). Here, a combined dataset incorporating morphological characters from both Decker & Wozencraft (1991) and Baskin (2004) offers a test of whether over-weighting dental characters or homoplasy affected previous results. Thus, a more complete understanding of the craniodental evolution within Procyonidae is needed to truly explore the conflict between morphology and molecules.

My analysis incorporated high-resolution X-ray computed tomography (HRXCT), updated computational methods for phylogenetic analyses, and a more thorough investigation of cranial anatomy, particularly of the auditory region. The primary goals of this analysis were to provide detailed descriptions of previously discussed craniodental characters, compile an updated and comprehensive morphological dataset, and generate a revised morphological phylogeny of the generic relationships within Procyonidae. A subsequent goal was to examine the morphological evolution within the family and to compare my phylogenetic results with recent molecular results in order to identify any morphological support for the molecular hypothesis of procyonid relationships.

## MATERIAL AND METHODS

The morphological dataset used here to evaluate relationships within Procyonidae included a total of 78 characters for 15 ingroup and five outgroup taxa (Appendix 1). Eleven characters were parsimony uninformative when including all taxa and characters. In the phylogenetic dataset, 64 characters were binary and 14 were multi-state; no characters were ordered. Of the 78 morphological characters, 35 were craniomandibular and 43 were dental. Twelve extant taxa and eight extinct taxa were included in the parsimony analysis using PAUP\*4.0b10 (Swofford, 2002). All extant taxa were scored based on direct observations of specimens. The majority of the fossils were scored from the literature and based on written anatomical descriptions, figures, and the author's character states. However, my state scores occasionally differed from the original author's because some aspect of the description, figure, or character state was not in agreement.

### TAXON SAMPLING

The species-exemplar approach (Wiens, 1998; Prendini, 2001) was employed for each extant procyonid genus

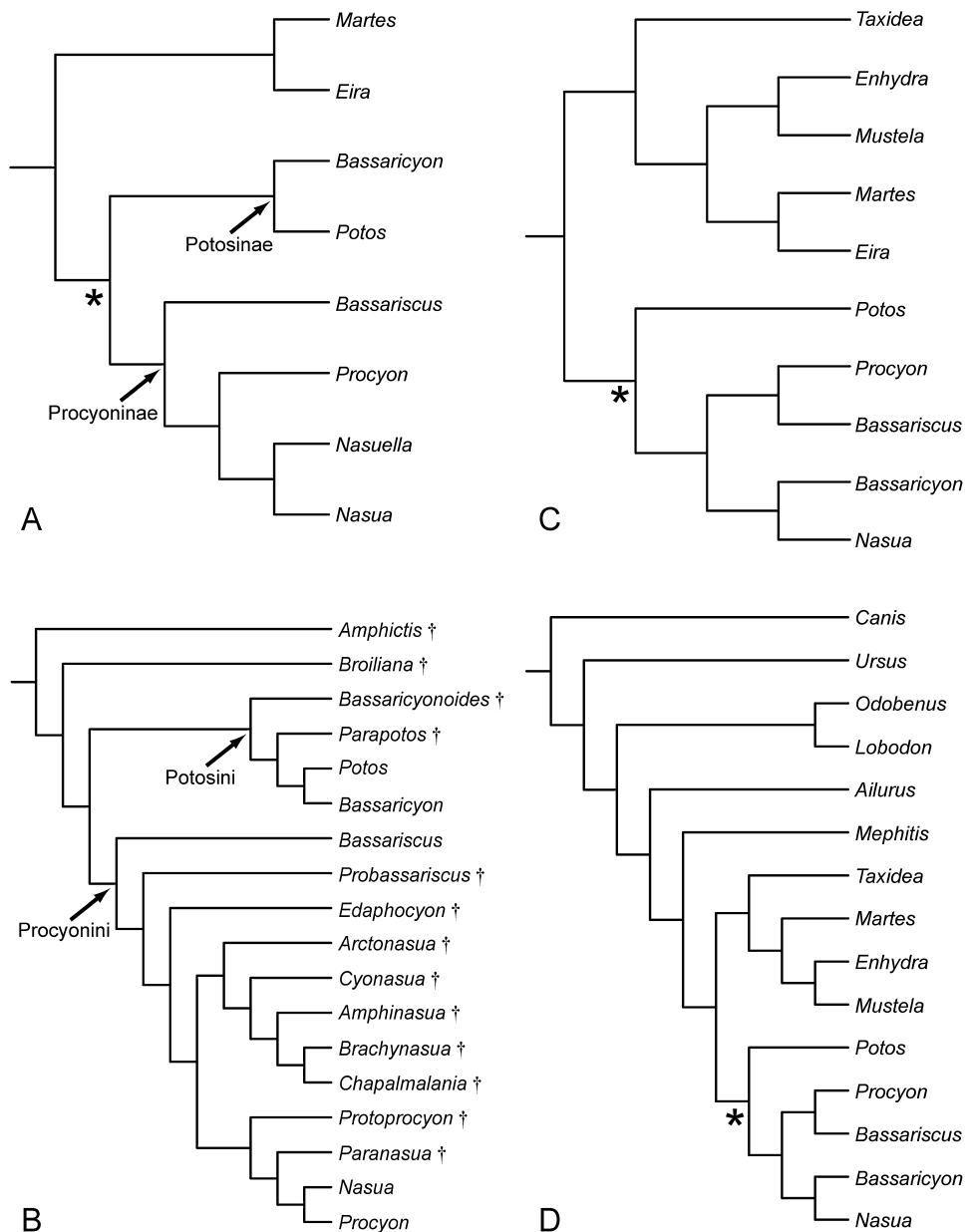


**Figure 1.** Phylogenetic hypotheses based on morphology recovered by: A, Decker & Wozencraft (1991) and B, Baskin (2004). Phylogenetic hypotheses based on molecular data recovered by: C, Koepfli *et al.* (2007) and D, Fulton & Strobeck (2007). Asterisk denotes Procyonidae, as defined by the author. Extinct taxa denoted by a dagger (†).

and several extinct procyonid genera; specimens examined are listed in Appendix 2. Previously, genera were scored as composite taxa (Baskin, 2004), which can lead to problems with individual character scoring and misleading phylogenetic results (Wiens, 1998; Prendini, 2001; Brusatte, 2010). Ingroup taxa included seven extant procyonid species representative of each genus. As some species of Procyonidae are rare in collections, only *Nasua* is represented by more than

one species. Seven extinct procyonid genera were included, each represented by a single exemplar except for *Arctonasua*, which was represented by two species. All of the fossils, except *Edaphocyon pointblankensis* (TMM 31190–76), were scored from the literature because of lack of access to specimens. The literature used to score each taxon is presented in Appendix 3. Fossils were selected on the basis of relative completeness and availability of published figures.

The species-exemplar approach was also used for the outgroup taxa. As it is best practice to include more than one outgroup (Maddison, Donoghue & Maddison, 1984), five caniform outgroup taxa were selected, including a canid (*Urocyon cinereoargenteus*), two mephitids (*Mydaus javanensis* and *Conepatus leuconotus*), a mustelid (*Martes pennanti*), and the ailurid, *Ailurus fulgens*. Although the relationships within Musteloidea are well studied, they remain relatively unresolved (Wyss & Flynn, 1993; Drago & Honeycutt, 1997; Bininda-Emonds *et al.*, 1999; Flynn *et al.*, 2000, 2005; Fulton & Strobeck, 2006; Eizirik *et al.*, 2010). *Ailurus fulgens* was included as an outgroup taxon, despite its controversial phylogenetic position (Wang, 1997; Bininda-Emonds *et al.*, 1999; Flynn *et al.*, 2000; Sato *et al.*, 2009). Thus, at least one representative from each musteloid family was included. *Urocyon cinereoargenteus* was incorporated to aid in optimization of the ancestral character states further outside of Musteloidea.

#### INSTITUTIONAL ABBREVIATIONS

F:AM, Frick Collection, American Museum of Natural History; FMNH, Field Museum of Natural History; KUVP, University of Kansas Natural History Museum; LACM, Los Angeles County Museum; MVZ, Museum of Vertebrate Zoology, University of California, Berkeley; ROM, Royal Ontario Museum; TMM, Vertebrate Paleontology Laboratory, Texas Natural Science Center, The University of Texas at Austin; UCLA, The UCLA Donald R. Dickey Bird and Mammal Collection, University of California, Los Angeles; UF, Florida Natural History Museum, University of Florida; USNM, National Museum of Natural History.

#### CHARACTERS

Character coding methods have been the subject of debate and controversy as different methods can result in different phylogenetic results. Two valid approaches are typically advocated in the literature but neither is without shortcomings; these methods are reductive and composite coding (Hawkins, Hughes & Scotland, 1997; Strong & Lipscomb, 1999; and references therein). Here, I scored characters using the reductive coding method because it generally reduces both poor primary homology assessments and error related to missing data in multi-state characters (Hawkins *et al.*, 1997; Strong & Lipscomb, 1999). The initial assessment of primary homology is crucial to phylogenetic analyses, and to equate colour, size, or shape of a trait with the presence or absence of that trait as required by the composite method is

nonhomologous (Hawkins *et al.*, 1997). A weakness of the reductive coding method, however, is the inclusion of logically dependent characters in a dataset (Strong & Lipscomb, 1999). Although composite coding does not incorporate logically dependent characters, it can lead to spurious results by rendering inapplicable data informative (Strong & Lipscomb, 1999) and recover homoplasy because of inappropriate homology assumptions (Hawkins *et al.*, 1997). Character states should be homologous, independent, and nonredundant (Pimentel & Riggins, 1987); unfortunately, both methods violate one of these requirements. I believe it is more important to preserve better assessments of primary homology than to eliminate instances of non-independent characters, and the reductive coding was used accordingly.

To ensure that the character coding method did not overly influence the results, I also ran the primary analysis using the composite coding method, combining characters 1 and 2, 6 and 7, 14 and 15, 23 and 24, 47 and 48, 51 and 52, 60 and 61, and 67 and 68. There was no difference in the resulting topology between the reductive and composite coding methods. It should also be noted that the accuracy of composite coding is affected when 'absence' of a trait is derived or when a secondary loss occurs (Strong & Lipscomb, 1999); both cases are present in the current dataset. Additionally, logical dependence of a character does not overweight those character states if one character defines a larger clade and the other defines one of its subclades (Strong & Lipscomb, 1999). Examination of the character matrix post hoc revealed that the logically dependent character pairs never diagnose the same clade.

All characters were run as unordered; only one character (29) exhibited possible evidence of a morphcline, which is a prerequisite for ordering characters (Slowinski, 1993). Additionally, parsimony uninformative characters, which were all autapomorphies, were included in the analyses because they represent instances of morphological evolution, although they do not aid in informing evolutionary relationships.

Characters were combined from the previous morphological analyses conducted by Decker & Wozencraft (1991) and Baskin (2004) to construct the most comprehensive dataset of craniodental morphological characters to date. Seven new characters were added to the combined morphological dataset. All characters are described and illustrated (Figs 2–34). Postcranial and soft-tissue characters, which were only incorporated by Decker & Wozencraft (1991), were not analysed for this study.

Computed tomography was utilized to better investigate characters of the auditory region and other internal areas of the cranium. Skulls from each

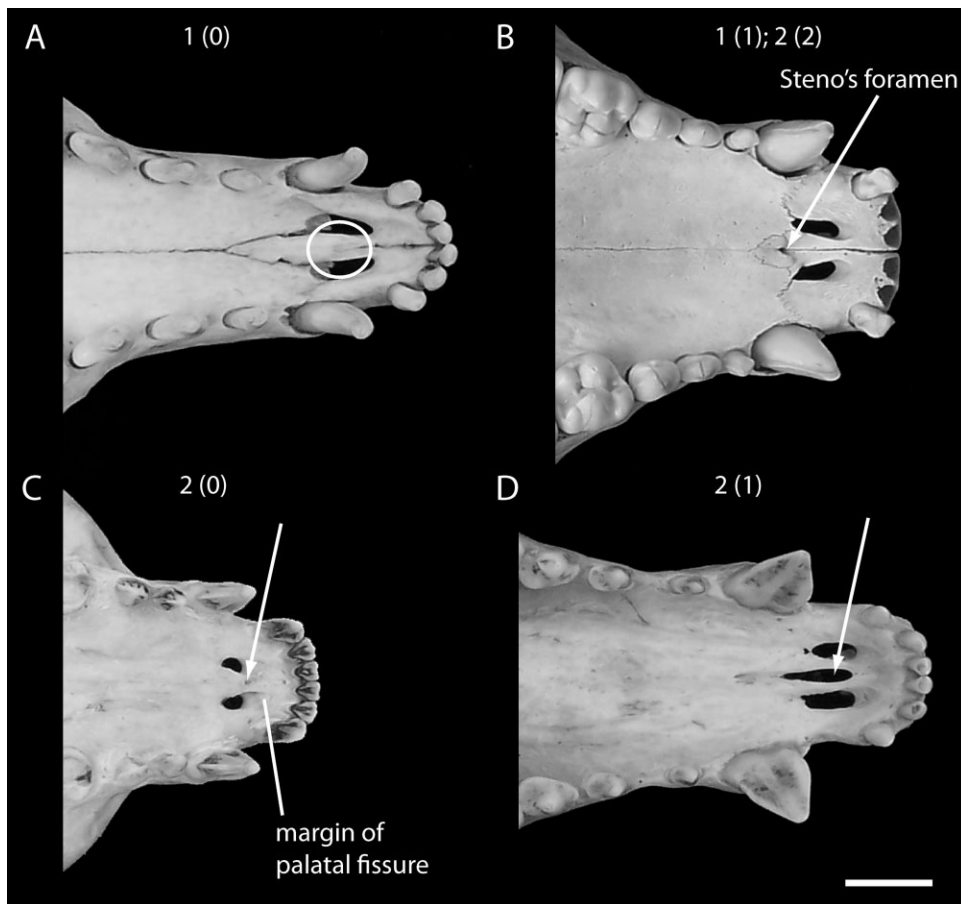


**Figure 2.** Characters 1 and 2. Ventral view of rostrum, anterior to the right. A, *Urocyon cinereoargenteus* MVZ 114285; B, *Procyon lotor* TMM 778; C, *Potos flavus* MVZ 155212; D, *Nasua narica* FMNH 14471. Circle: absence of Steno's foramen. See text for character descriptions and states. Scale bar = 1 cm.

extant genus, except *Conepatus*, were scanned at The University of Texas HRXCT Facility. Scan data were then resliced and three-dimensional models rendered using VGStudioMax v. 2.0.1 (Volume Graphics, Heidelberg, Germany). The scanning parameters of each specimen are presented in Appendix 4.

#### PHYLOGENETIC ANALYSES

The dataset was analysed using PAUP\*4.0b10 (Swofford, 2002). A series of taxon addition-deletion runs was performed in order to explore different signals within the overall dataset. All trees were rooted with the outgroup paraphyletic with respect to the ingroup. Because of the smaller size of the dataset, parsimony analysis of the 12 extant taxa was performed using an exhaustive search. All other parsimony analyses used heuristic searches with tree-bisection reconnection (TBR) branch swapping and 100 000 random-addition-sequence replicates. Strict consensus trees were produced for each analysis with

more than one most parsimonious tree (MPT). Tree length, consistency index (CI), retention index (RI), and rescaled consistency index (RC) were computed for each most parsimonious tree. Bremer decay support indices were computed using PAUP\*4.0b10. Taxa with multistate characters were interpreted as ambiguities.

The analysis of all 13 taxa personally observed, which includes 12 extant taxa plus the extinct *Edaphocyon pointblankensis*, is the primary analysis (Fig. 35). This analysis was used to describe character distributions and polarity, as well as to trace character evolution. MacClade 4 (Maddison & Maddison, 2005) was used to map character transformations on both the morphological and molecular tree topologies.

## RESULTS

### CRANIAL CHARACTERS

1. Steno's foramen: (0) absent; (1) present, Figure 2 (modified from Decker & Wozencraft, 1991).

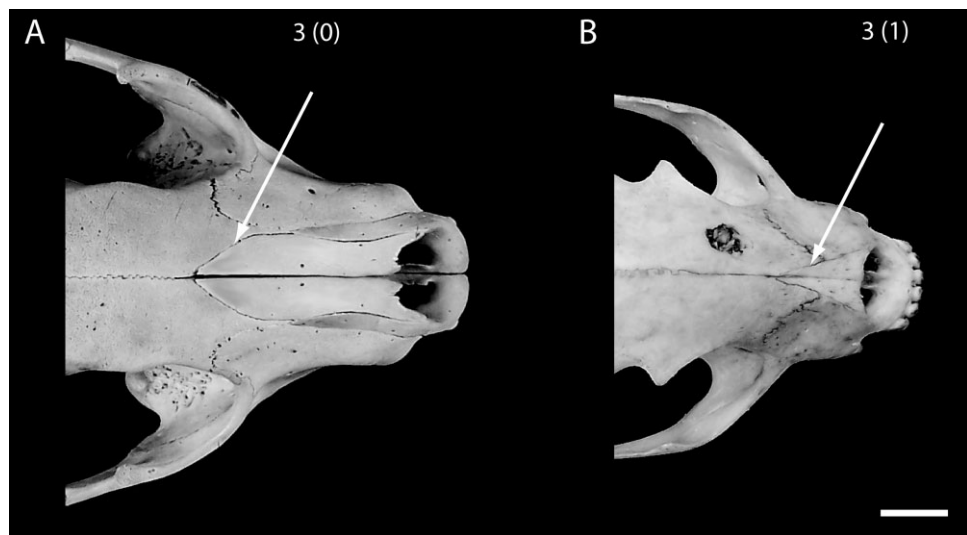


**Figure 3.** Character 3. Dorsal view, anterior to the right. A, *Procyon lotor* TMM 778; B, *Potos flavus* MVZ 155212. White arrow: posterior margin of nasals. Scale bar = 1 cm.

Steno's foramen, when present, is completely enclosed between the premaxillae and transmits the median septal artery. Previously, the primitive state was described as 'lost or vestigial' and the derived state as 'present, large' (Decker & Wozencraft, 1991). I simplified the character to absent or present because Steno's foramen is invariably present within Procyonidae.

**Distribution and polarity:** Only *Urocyon cinereoar- genteus* exhibits state (0); thus, the presence of Steno's foramen is plesiomorphic for Procyonidae.

2. Steno's foramen, shape: (0) anterior and posterior margins between palatal fissures; (1) anterior margin between palatal fissures, posterior margin caudal to palatal fissures; (2) anterior margin at or caudal to posterior margin of palatal fissure, posterior margin caudal to palatal fissures, Figure 2 (modified from Decker & Wozencraft, 1991).

I combined two separate characters from Decker & Wozencraft (1991) that deal with the size and shape of Steno's foramen. One character referred to the presence or absence and size of the foramen (lost or vestigial and present, large), whereas another referred to the placement and position of the foramen (on posterior edge of incisive foramina and between incisive foramina; Decker & Wozencraft, 1991). However, the two characters are not necessarily independent. For instance, Steno's foramen in *Nasua* is large and extends from between the palatal fissures (=incisive foramina) posteriorly, such that it terminates caudal to the posterior margins of the palatal fissures. In taxa having a small and circular Steno's foramen, the entire foramen is either between the

palatal fissures, or the anterior margin of the foramen is at or caudal to the posterior margin of the palatal fissures.

**Distribution and polarity:** The ancestral state cannot be reconstructed unequivocally. State (0) is present in *Mydaus javanensis*, *Bassariscus astutus*, and at node 8 (Fig. 35). State (1) is the derived condition for node 11. *Conepatus leuconotus*, *Martes pen- nanti*, and *Procyon lotor* independently derive the posteriorly shifted condition of Steno's foramen (state 2).

3. Nasals, posterior margin: (0) broad articulation with frontals; (1) narrow articulation with frontals, Figure 3 (modified from Decker & Wozencraft, 1991).

The posterior margin of the nasals either contacts the frontals by means of a broad, U-shaped or V-shaped articulation (state 0), or by a narrow V-shaped articulation (state 1). In taxa having the narrow articulation, the nasals uniformly taper posteriorly; in taxa having the broad articulation between the nasals and frontals, the nasals remain relatively uniform in width until tapering to a broad posterior angle. As originally described, the primitive state of the character was 'U-shaped' (Decker & Wozencraft, 1991); however, that minimal description does not adequately encompass the primitive state because some taxa, such as *Nasua narica*, exhibit a broad V-shaped articulation, rather than a U-shaped posterior margin.

**Distribution and polarity:** The primitive condition for Procyonidae is a broad articulation between the

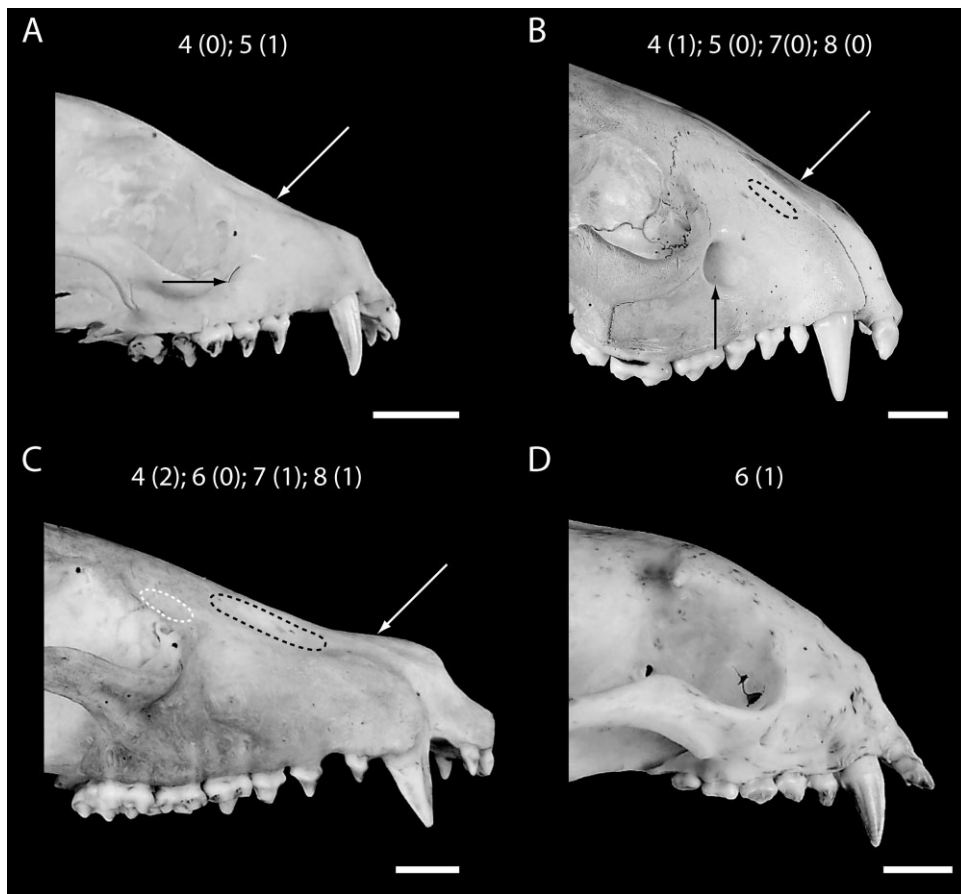


**Figure 4.** Characters 4, 5, 6, 7, and 8. Right lateral view, anterior to the right. A, *Bassaricyon alleni* FMNH 65788; B, *Procyon lotor* TMM 778; C, *Nasua narica* FMNH 14471; D, *Potos flavus* MVZ 132125. White arrow: dorsal surface of nasal; black arrow: ventral border of infraorbital foramen; black dashed line: outline of nasolabialis fossa; white dashed line: outline of antorbital fossa. Scale bars = 1 cm.

nasals and frontals (state 0); with state (1) derived independently in *Mydaus javanensis*, *Potos flavus*, and *Nasuella olivacea*.

4. Nasal, dorsal surface in lateral view: (0) straight; (1) slightly concave; (2) strongly concave and upturned anteriorly, Figure 4 (modified from Decker & Wozencraft, 1991).

In lateral view, the dorsal surface of the nasal either exhibits a straight profile (state 0), slightly concave profile (state 1), or the nasal is so strongly concave that it trends dorsally towards the external nares (state 2). The latter condition seems to correlate with other features of the snout in the coatis, such as the elongated rostrum and flexible snout (Decker & Wozencraft, 1991). I added a third state to the original character that differentiates between taxa that have a truly straight nasal in lateral profile and one that is slightly concave. These states were both previously scored as ‘straight’ (Decker & Wozencraft, 1991).

Distribution and polarity: The ancestral condition for Procyonidae is state (1). Under the new scoring for this character, only *Bassaricyon alleni* and *Potos flavus* exhibit the straight condition, which is derived for node 9. Both *Nasuella* and *Nasua* exhibit the strongly concave and upturned anteriorly nasal condition (state 2), which is derived at node 11.

5. Infraorbital canal: (0) ventral and dorsal borders in line; (1) ventral border posterior to dorsal border, Figure 4 (Decker & Wozencraft, 1991).

The infraorbital canal transmits the infraorbital vessels and nerve of the maxillary branch of the trigeminal nerve (CN V). The ventral border of the canal often is defined by a small, anteriorly extending ridge; when the ridge is absent, the ventral border is defined by the ventral termination of the opening. There is a distinct difference between the morphology described in state (0) and state (1). Some minor variation in the position of the ventral border exists, particularly in *Procyon lotor*. The ventral border of the

infraorbital canal can be immediately posterior to the dorsal border; however, it is not the same condition as state (1).

Distribution and polarity: State (0) is the primitive condition for Procyonidae. State (1) is derived in *Conepatus leuconotus* and at node 8.

6. Nasolabialis fossa: (0) present; (1) absent, Figure 4 (Decker & Wozencraft, 1991).

The nasolabialis fossa lies along the dorsal extent of the maxilla, just ventral to the contact between the maxilla and nasal. The nasolabialis fossa serves as the attachment site for the maxillonasolabialis muscle, which aids in movement of the rhinarium (Decker & Wozencraft, 1991). The fossa is subtle in most taxa, such as *Ailurus fulgens*, where only a very shallow fossa is present. The character and taxon scoring was consistent with that of Decker & Wozencraft (1991).

Distribution and polarity: State (0) is the ancestral condition for Procyonidae. State (1) is derived in *Conepatus leuconotus* and at node 9.

7. Nasolabialis fossa size: (0) shallow; (1) deep, Figure 4.

The nasolabialis fossa is either shallow (state 0) or deep (state 1). When the nasolabialis fossa is shallow it may be relatively difficult to distinguish, as in *Ailurus fulgens*. However, when deep, the nasolabialis fossa is better defined and more apparent.

Distribution and polarity: State (0) is the plesiomorphic condition for Procyonidae whereas state (1) is present in *Nasua nasua* and *Nasua narica* and derived for node 12.

8. Antorbital fossa: (0) absent or small; (1) present, deep, Figure 4 (modified from Decker & Wozencraft, 1991).

The antorbital fossa is located on the articulation between the lacrimal and maxilla, just ventral to the articulation of the frontal with those bones. The fossa is either absent or small (state 0) or present and deep (state 1). The character was modified from its original form (Decker & Wozencraft, 1991) by substituting 'small' for the term 'vestigial' because 'vestigial' implies an evolutionary history a priori. Additionally, state zero was not divided into additional states because the fossa may be so small that its presence is ambiguous.

Distribution and polarity: State (0) is the ancestral condition for Procyonidae. The derived state (1) is present in *Martes pennanti*, *Ailurus fulgens*, and at node 11.

9. Palate, posterior extent: (0) to the level of the last upper molar; (1) just posterior to the last upper

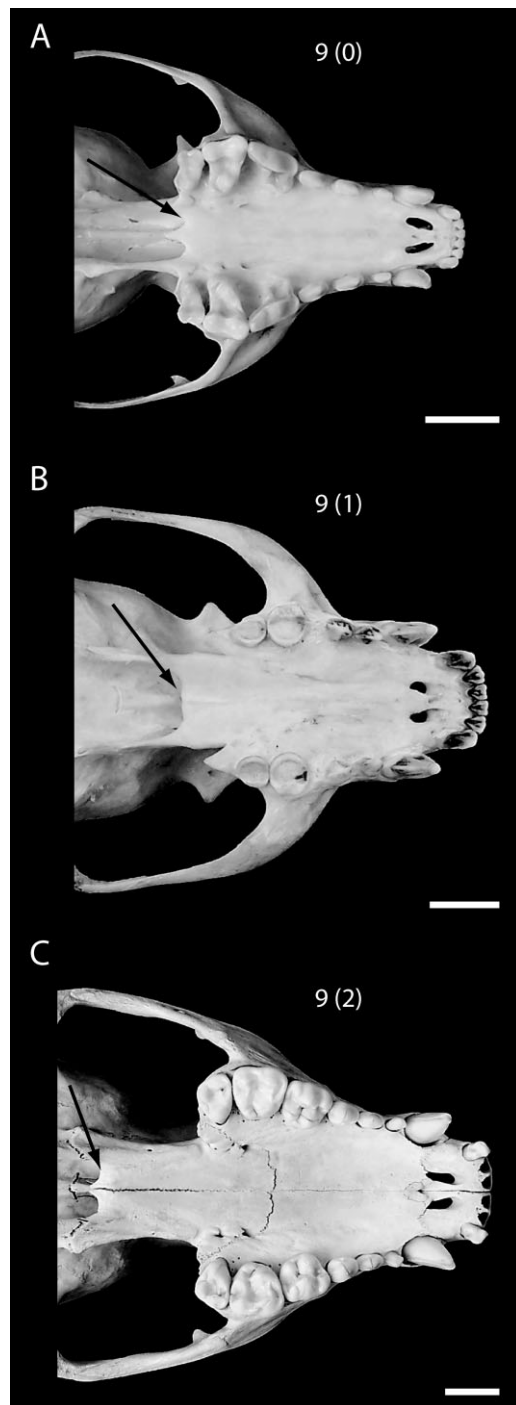


**Figure 5.** Character 9. Ventral view, anterior to the right. A, *Bassariscus astutus* MVZ 192085; B, *Potos flavus* MVZ 155212; C, *Procyon lotor* TMM 778. Black arrow: posterior extent of palate. Scale bars = 1 cm.

molar; (2) well posterior of the last upper molar, Figure 5 (modified from Baskin, 2004: character 7).

The hard palate consists posteriorly of the ventral horizontal lamina of the palatine, which is exposed in



**Figure 6.** Character 10. Ventral view, anterior to the right. A, *Nasua narica* FMNH 14471; B, *Potos flavus* MVZ 132125. Black arrow: inflation of the orbital wall. Scale bars = 1 cm.

ventral view. The ventral horizontal lamina extends to different lengths, delineated by the posterior edge of that lamina with respect to the last upper molar. I changed the reference point to the last upper molar from M2 in the original character description (Baskin, 2004), so that the character was relevant to outgroup taxa in which the second upper molar is lost. In taxa with only one upper molar, the posterior extent of the palatine exhibits variable states, suggesting that the loss of M2 does not impact the scoring of this character.

**Distribution and polarity:** The plesiomorphic condition for Procyonidae is state (2). State (0) is present in *Urocyon cinereoargenteus* and *Bassariscus astutus*. State (1) is independently derived in *Conepatus leuconotus*, *Ailurus fulgens*, and *Potos flavus*.

10. Palatine, inflation of the orbital wall: (0) inflated; (1) diverging, not inflated, Figure 6 (modified from Decker & Wozencraft, 1991).

The perpendicular lamina of the palatine, or lateral wall of Decker & Wozencraft (1991), extends from the ventral horizontal lamina dorsally where it articulates with the frontal and sphenoid bones. The wall is often expanded laterally such that the perpendicular lamina is concave. There is often a triangular process, which extends posterolaterally from the caudal end of

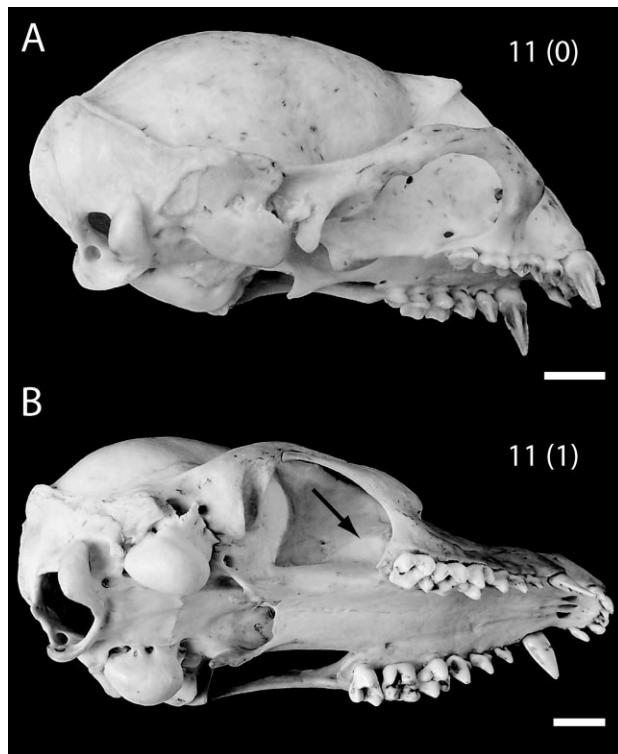


**Figure 7.** Character 11. Right ventrolateral view, anterior to the right. A, *Potos flavus* MVZ 132125; B, *Nasua narica* FMNH 14013. Black arrow: zygomaticaus muscular fossa. Scale bars = 1 cm.

the perpendicular lamina. That expansion causes the orbital wall to appear inflated (Decker & Wozencraft, 1991). Originally, the inflated state was considered derived for Procyoninae, with state (0) defined as ‘diverging, not inflated’ and state (1) as ‘inflated’ (Decker & Wozencraft, 1991).

**Distribution and polarity:** The ancestral condition for Procyonidae is state (0). State (1) is derived in *Urocyon cinereoargenteus* and at node 9.

11. Deep zygomaticus muscle fossa in orbital wall: (0) absent; (1) present, Figure 7 (Decker & Wozencraft, 1991).

A deep fossa for the zygomaticus muscle is either absent (state 0) or present (state 1) on the medial wall of the orbit. When present, the fossa is distinct and located anteriorly along the perpendicular lamina. The dorsal margin of the zygomaticus muscle fossa is marked by a ventrally concave ridge. The character and character states were retained from Decker & Wozencraft (1991).

**Distribution and polarity:** The ancestral condition for Procyonidae is state (0). State (1) is derived independently in *Urocyon cinereoargenteus* and at node 12.



**Figure 8.** Characters 12, 13, 14, and 15. Ventral view, anterior to the right. A, *Urocyon cinereoargenteus* MVZ 114285; B, *Procyon lotor* TMM 778; C, *Potos flavus* MVZ 155212; D, *Nasua nasua* FMNH 70728. Black dashed line: outline of concavity of the palate; white arrow: maxillopalatine suture; black arrow: nasal spine. Scale bars = 1 cm.

12. Palatine, bony palate: (0) flat; (1) slightly concave, Figure 8 (modified from Decker & Wozencraft, 1991).

The medial contact between the palatines is either flat (state 0) or slightly concave dorsally (state 1). In most taxa, the depression is bound on all sides, and the posterior edge of the palatines turn ventrally caudal to the depression. The palatines of *Potos flavus* slope dorsally to the posterior margin without turning ventrally again; this condition was scored as concave. Character 12 here corresponds to Decker & Wozencraft's (1991) mesopterygoid region character: 'flat or absent' or 'slightly concave'. The mesopterygoid region of Decker & Wozencraft (1991) seems to be the area composed of the palatines posterior to the last upper molar. As the depression can extend anterior to the last upper molar, I emended the character to refer to the entire bony palate instead of the more restricted mesopterygoid region. Additionally, the absence of a mesopterygoid region is represented by character 9, state (2) in my analysis. This character is also corre-

lated with another character of Decker & Wozencraft (1991): mesopterygoid region: 'present' or 'absent'.

Distribution and polarity: State (0) is the plesiomorphic condition for Procyonidae with state (1) derived independently at node 3, node 10, and in *Potos flavus*.

13. Maxilla–palatine suture: (0) U-shaped; (1) truncate, Figure 8 (Decker & Wozencraft, 1991).

The articulation between the maxillae and the palatines is either strongly U-shaped (state 0) or more truncate and squared off (state 1). The character and character states were retained from Decker & Wozencraft (1991). The condition in *Ailurus fulgens* is ambiguous because the suture is almost completely fused in the specimen examined.

Distribution and polarity: State (0) is the primitive condition for Procyonidae, with state (1) derived only in *Procyon lotor*.

14. Nasal spine: (0) present; (1) absent, Figure 8.

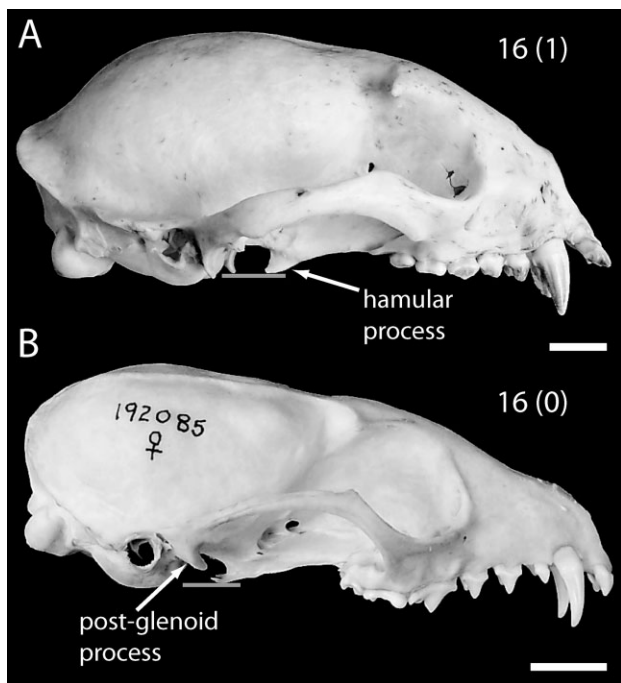


**Figure 9.** Character 16. Right lateral view, anterior to the right. A, *Potos flavus* MVZ 132125; B, *Bassariscus astutus* MVZ 192085. Grey line: dorsal plane. Scale bars = 1 cm.

The nasal spine is either present (state 0) or absent (state 1). The nasal spine, when present, projects posteriorly from the caudal margin of the palatines at the floor of the nasopharyngeal meatus. The nasal spine exhibits two different morphologies (see character 15).

Distribution and polarity: State (0) is ancestral for Procyonidae. The nasal spine is independently lost in *Mydaus javanensis*, *Ailurus fulgens*, *Potos flavus*, *Nasuella olivacea*, and *Nasua narica*. This character is one of the few that differentiate the two species of *Nasua*, but it is not informative for relationships within Procyonidae.

15. Nasal spine, shape: (0) triangular; (1) rounded, Figure 8.

The nasal spine is either sharply triangular (state 0) or blunt and rounded (state 1). When the spine is rounded it also tends to be much wider than the triangular nasal spines.

Distribution and polarity: State (0) is the plesiomorphic state when the nasal spine is present, whereas state (1) is an autapomorphy for *Nasua nasua*.

16. Hamular process of the pterygoid: (0) extends below horizontal plane of postglenoid process; (1) lies in same plane, Figure 9 (Decker & Wozencraft, 1991).

The hamular process of the pterygoid, which projects posteriorly, either projects ventral to the postglenoid process in the dorsal plane (state 0) or lies in the same plane medial to the postglenoid process (state 1). The character and scorings were consistent with the original interpretation (Decker & Wozencraft, 1991).

Distribution and polarity: State (0) is the ancestral condition for Procyonidae. State (1) is exhibited only in *Potos flavus* and is an autapomorphy of the taxon.

17. Vomer, posterior extent and attachment to palate: (0) attached to anterior part of palate only; (1) attached to anterior and posterior part, Figure 10 (modified from Decker & Wozencraft, 1991).

The vomer lies within the nasal cavity and comprises much of the median partition and some of the dorsal boundary of the nasopharyngeal meatus. All taxa have an anterior attachment of the vomer, but in some taxa the vomer extends posteriorly towards the posterior margin of the palatine where it articulates with the palatine. State (1) is recognized if the posterior extent of the vomer is visible within the nasopharyngeal meatus. In those taxa where the vomer only attaches to the anterior part (state 0) of the palate, the nasopharyngeal meati share a common opening posteriorly. This character is somewhat ambiguous in *Bassariscus astutus*, where the vomer extends posteriorly but does not attach at the caudal margin of the palatines. Thus, the vomer does not continue as far caudally as in *Procyon lotor* and *Nasua nasua*, but can still be observed within the nasopharyngeal meatus. This character remained similar to the original character (Decker & Wozencraft, 1991); it has been revised to be more anatomically explicit. Scoring was congruent with that of Decker & Wozencraft (1991).

Distribution and polarity: The ancestral state for Procyonidae cannot be reconstructed unequivocally. State (0) is present in *Urocyon cinereoargenteus*, *Martes pennanti*, and at node 8. State (1) is present at node 3, in *Bassariscus astutus*, and at node 10.

18. Rostral process of lacrimal: (0) absent; (1) present, Figure 11 (Decker & Wozencraft, 1991).

The lacrimal, which makes up part of the anterior margin of the orbit, may possess a rostral process. The rostral process is an anterior projection beyond the orbital rim (state 1). I scored *Bassaricyon alleni* as possessing a rostral process, which Decker & Wozencraft (1991) scored as absent. The sutures between the lacrimal and the surrounding bones fuse relatively early compared to other sutures, so the rostral process often is difficult to distinguish in mature specimens.

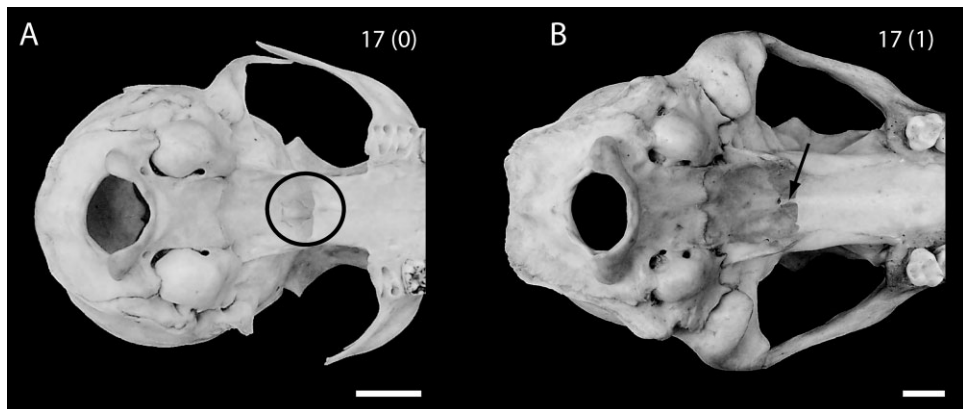


**Figure 10.** Character 17. Posteroventral view, anterior to the right. A, *Bassaricyon alleni* FMNH 65788; B, *Nasua narica* FMNH 14471. Black circle: absence of posterior extent of vomer; black arrow: posterior extent of vomer. Scale bars = 1 cm.

Distribution and polarity: State (0) is the primitive state for Procyonidae. State (1) is observed in *Bassaricyon alleni*, *Nasua nasua*, *Nasua narica*, and *Nasuella olivacea*. The rostral process is independently derived in *Bassaricyon alleni* and at node 11.

19. Naso-lacrimal foramen: (0) fossa for the lacrimal gland and canal for the lacrimal duct well developed; (1) fossa reduced and canal absent, Figure 11 (modified from Decker & Wozencraft, 1991).

The naso-lacrimal foramen lies within the lacrimal along the orbital rim near the articulation of the lacrimal with the jugal and maxilla; tracking anteroventrally from the foramen is the naso-lacrimal canal. The foramen and canal are usually well developed (state 0), but those structures may be reduced to absent (state 1). The orbital wall of *Potos flavus* is relatively thin; thus there is no distinct naso-lacrimal duct and the canal is absent (Decker & Wozencraft, 1991). The character scoring was congruent with the original discussion of the character (Decker & Wozencraft, 1991).

Distribution and polarity: State (1) is derived only in *Potos flavus* and is an autapomorphy of that taxon.

20. Lambdoidal ridge: (0) extends to mastoid; (1) continuous with zygomatic arch, Figure 12 (Decker & Wozencraft, 1991).

The lambdoidal ridge, which runs from the midline of the occipital ventrolaterally along the posterior margin of the parietal, either terminates on the mastoid process of the temporal bone (state 0) or at the posterior end of the zygomatic arch (state 1). The character and states were retained from Decker & Wozencraft (1991).

Distribution and polarity: State (0) is the ancestral condition for Procyonidae. State (1) is independently

derived in both *Urocyon cinereoargenteus* and *Potos flavus*. This character was considered an autapomorphy of *Potos flavus* by Decker & Wozencraft (1991); however, the inclusion of *Urocyon cinereoargenteus* indicates that state (1) is rather an autapomorphy within Procyonidae.

21. Sagittal crest, males: (0) present; (1) absent, Figure 12 (Decker & Wozencraft, 1991).

The sagittal crest, when present (state 0), lies along the midline extending from the interparietal anteriorly. The presence and size of the sagittal crest are correlated with age and sex of the individual. The character and character states were retained from Decker & Wozencraft (1991).

Distribution and polarity: State (0) is plesiomorphic for Procyonidae. State (1) is exhibited independently in both *Nasuella olivacea* and *Urocyon cinereoargenteus*. Decker & Wozencraft (1991) identified the absence of a sagittal crest in males as an autapomorphy of *Nasuella olivacea*; however, scoring of an additional outgroup (*Urocyon cinereoargenteus*) suggests that state (1) is a local autapomorphy for *Nasuella olivacea* within Procyonidae.

22. Alisphenoid canal: (0) present; (1) absent, Figure 13 (Baskin, 2004: character 2).

The alisphenoid canal (present, state 0) is formed by the alisphenoid bone (Evans, 1993) and houses the internal maxillary artery (Story, 1951). The foramen ovale, which transmits the mandibular branch of the trigeminal nerve (CN V), either opens into the alisphenoid canal or into the orbit when the alisphenoid canal is absent (state 1). The absence of an alisphenoid canal has previously been considered either diagnostic of Procyonidae (Turner, 1848) or of *Broiliiana* and New World Procyoninae (Baskin, 2004). However, I recover the absence of the alisphenoid canal in *Urocyon cinereoargenteus*.

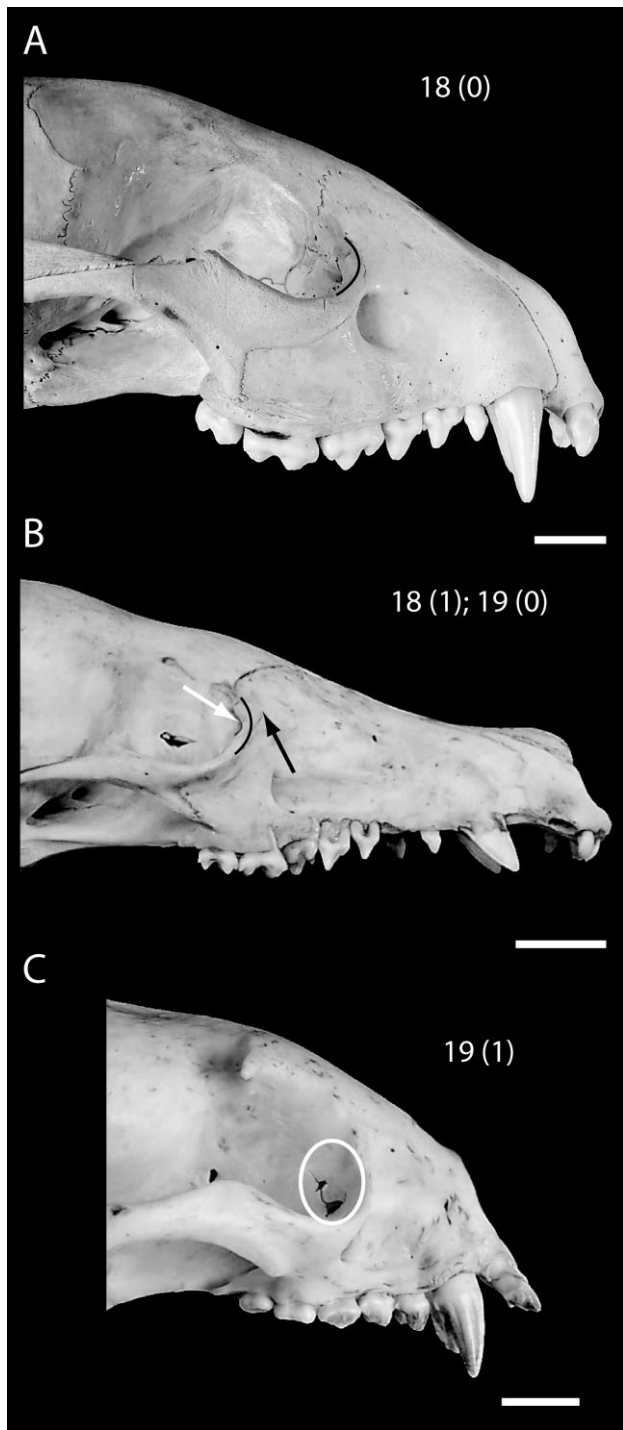


**Figure 11.** Characters 18 and 19. Right lateral view, anterior to the right. A, *Procyon lotor* TMM 778; B, *Nasuella olivacea* FMNH 70746; C, *Potos flavus* MVZ 132125. Black line: orbital rim; black arrow: rostral process; white arrow: fossa for the lacrimal gland; white circle: reduced fossa for the lacrimal gland. Scale bars = 1 cm.

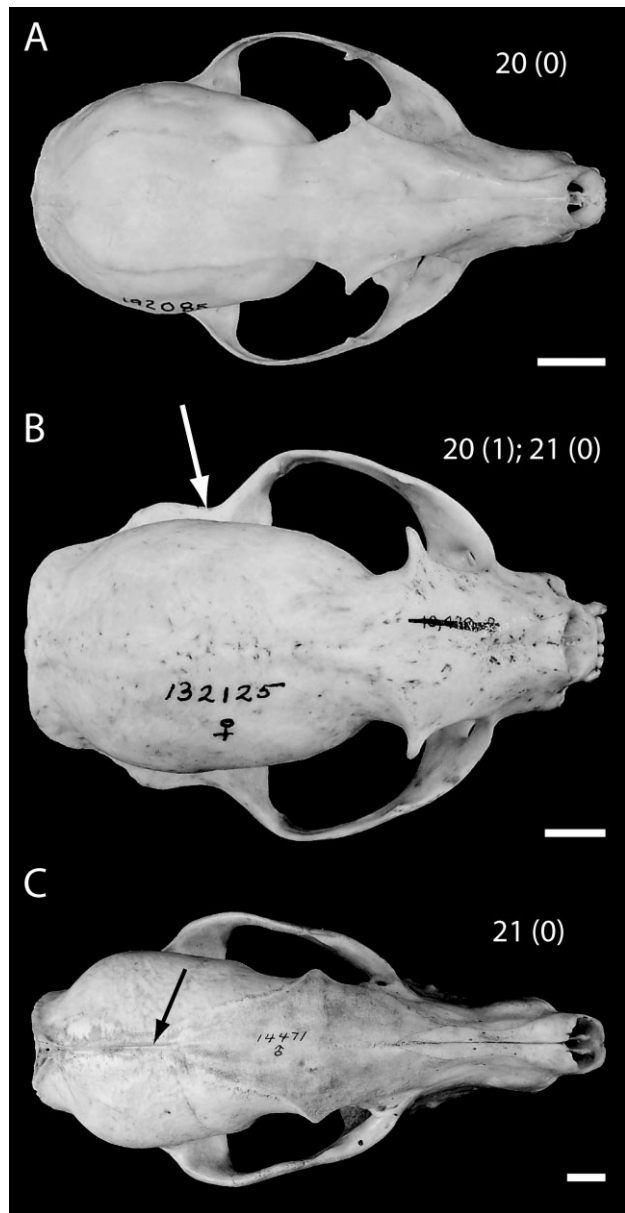


**Figure 12.** Characters 20 and 21. Dorsal view, anterior to the right. A, *Bassariscus astutus* MVZ 192085; B, *Potos flavus* MVZ 132125; C, *Nasua narica* FMNH 14471 (male). White arrow: anterior extension of the lambdoidal ridge; black arrow: sagittal crest. Scale bars = 1 cm.

noid canal is as a symplesiomorphy for Procyonidae. My character and states were consistent with that of Baskin (2004).

Distribution and polarity: State (0) is present in *Urocyon cinereoargenteus* and *Ailurus fulgens*. State (1) is derived at node 2.

23. Suprameatal fossa: (0) absent; (1) present, Figure 14 (modified from Baskin, 2004: character 1, Decker & Wozencraft, 1991).

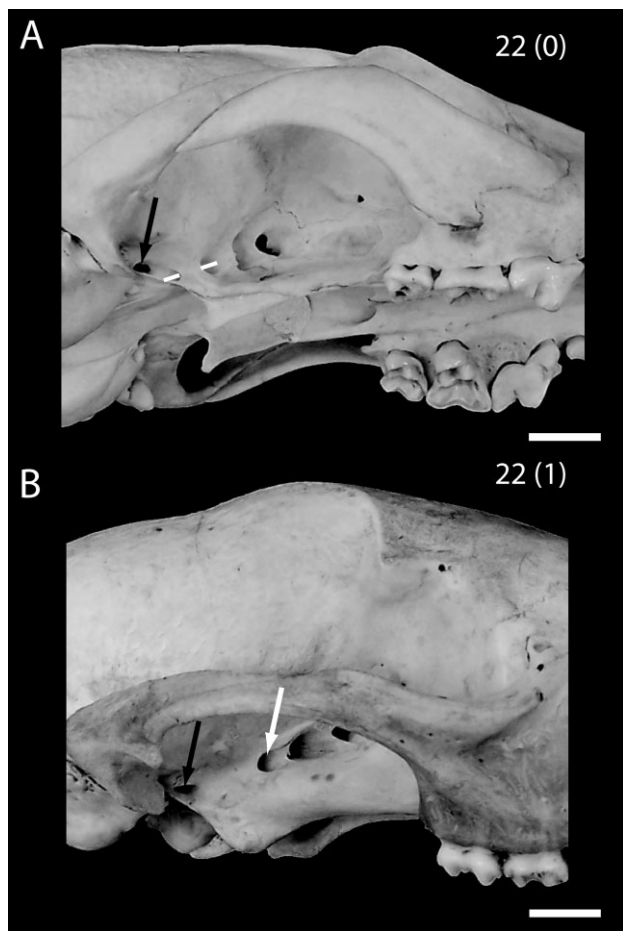


**Figure 13.** Character 22. A, *Urocyon cinereoargenteus* MVZ 114285, ventrolateral view; B, *Nasua narica* FMNH 14471, lateral view, anterior to the right. White line: through the alisphenoid canal; white arrow: foramen rotundum; black arrow: foramen ovale. Scale bars = 1 cm.

The suprrameatal fossa is an expansion in the roof of the external auditory meatus, which is composed of the squamosal. The suprarmeatal fossa is either absent (state 0) or present (state 1) with variable depths and orientations; the various morphologies of the fossa were included here as a separate character.

Distribution and polarity: State (0) is exhibited by *Urocyon cinereoargenteus*, *Mydaus javanensis*, and *Conepatus leuconotus*; the suprarmeatal fossa is secondarily lost in extant skunks (Wolsan, 1999). State (1) is derived at node 4.

24. Suprarmeatal fossa, size: (0) shallow; (1) deep, ventrally expanded lateral wall; (2) deep, dorsally expanded roof, Figure 14 (modified from Wolsan, 1993: character 9; modified from Baskin, 2004: character 1).

The morphology of the suprarmeatal fossa varies, such that it is either shallow (state 0), deep with a

ventrally expanded lateral wall (state 1), or deep with a dorsally expanded roof (state 2). A distinction has been made historically between a shallow suprarmeatal fossa and the deep conditions of the fossa (Schmidt-Kittler, 1981; Decker & Wozencraft, 1991; Wolsan, 1993; Baskin, 2004), with the shallow suprarmeatal fossa generally considered primitive for Musteloidea (Schmidt-Kittler, 1981). Although not present in extant mephitids, the fossa has been identified in extinct mephitids (Wolsan, 1999; Ahrens, 2009), which were not sampled for this analysis. The fossa may even be primitive for caniforms (Wang & Tedford, 1994; Baskin, 2004). Controversy has surrounded the interpretation of the morphology of the fossa in *Bassariscus*. Schmidt-Kittler (1981) described the suprarmeatal fossa in *Bassariscus astutus* as a highly developed procyonid condition, whereas Wolsan (1993) considered *Bassariscus astutus* to possess an intermediate mustelid stage and classified *Bassariscus* accordingly. Although *Bassariscus* does have a posterolaterally orientated fossa, compared to the more posteromedially orientated fossa in other procyonids (Decker & Wozencraft, 1991), I believe that the condition is more similar to other procyonids than mustelids, such as *Martes pennanti*. Additionally, use of HRXCT has shown that *Bassariscus astutus* has a fossa that is deep by means of a dorsally expanded roof, and thus the taxon was scored as possessing state (2). The character and character states were modified from Wolsan (1993) and Baskin (2004).

Distribution and polarity: State (0) is present in *Ailurus fulgens* and state (1) is present in *Martes pennanti*. The character state transformation from state (2) to state (0) in *Ailurus fulgens* requires a reversal to the primitive condition of the suprarmeatal fossa (Schmidt-Kittler, 1981). State (2) is derived at node 5, Procyonidae.

25. Epitympanic sinus: (0) present; (1) absent, Figure 14 (modified from Decker & Wozencraft, 1991).

The epitympanic sinus is a dorsally orientated extension of the epitympanic recess in the temporal bone and exhibits significant morphological variation amongst taxa. However, the scoring of this character differs herein from the original scoring (Decker & Wozencraft, 1991), which was probably based on broken skulls and isolated petrosals, rather than HRXCT, and may have led to the different interpretations. The incorporation of *Martes pennanti* and *Urocyon cinereoargenteus* reversed the polarity; thus state (0) is now presence of an epitympanic sinus. The variation in the morphology of the epitympanic sinus warrants more extensive evaluation and may constitute additional characters.

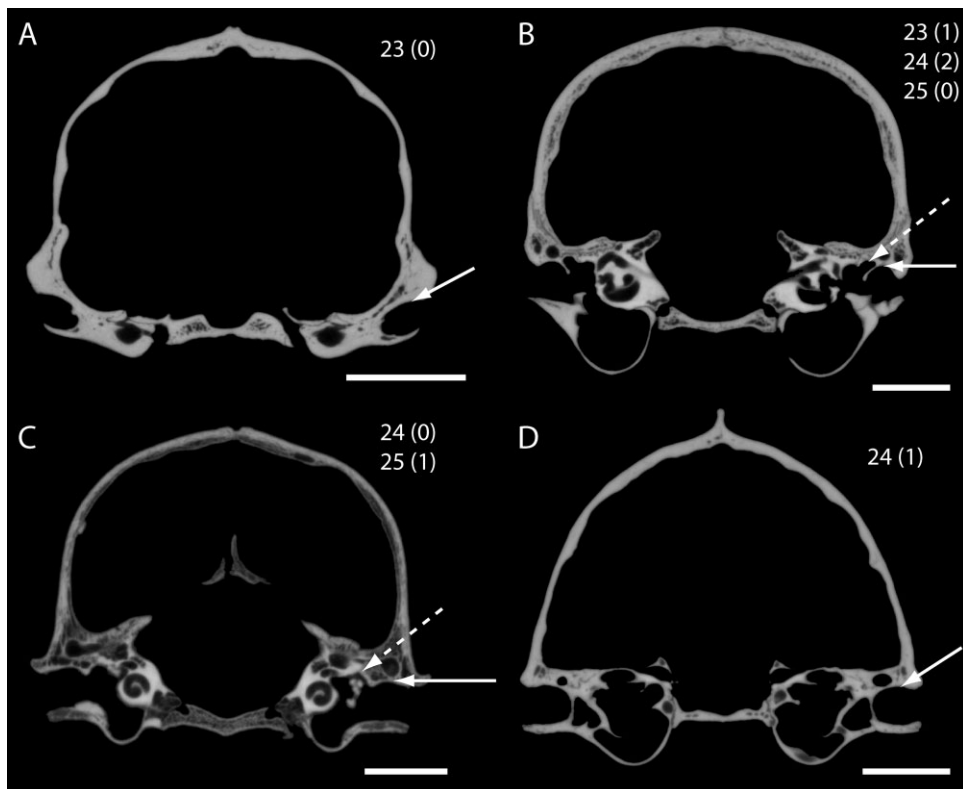


**Figure 14.** Characters 23, 24, and 25. Coronal slice, high-resolution X-ray computed tomography image. A, *Mydaus marchei* FMNH 62878 slice 582; B, *Procyon lotor* TMM 778 slice 559; C, *Ailurus fulgens* ROM 180 slice 481; D, *Martes pennanti* MVZ 29809 slice 559. Solid white arrow: characters 23 and 24; dashed white arrow: character 25. Scale bars = 1 cm.

Distribution and polarity: State (0) is the plesiomorphic state for Procyonidae. State (1) is independently derived in *Mydaus javanensis* and *Ailurus fulgens*.

26. Insertion of tensor tympani muscle: (0) deep, exposed fossa; (1) deep fossa, roofed by bony plate, Figure 15 (Decker & Wozencraft, 1991).

The tensor tympani muscle is located entirely within the tympanic cavity and aids in tensing the tympanic membrane (Evans, 1993). The muscle originates in the fossa for the tensor tympani, which is one of the largest fossae within the tympanic cavity, comparable in size to the epitympanic recess plus sinus. The fossa is either completely open to the tympanic cavity (state 0), or may be ‘roofed’ by a bony plate, which extends laterally from the ventromedial margin of the fossa (state 1). Note that when the petrosal is intact within the skull, the plate lies along the floor of the fossa, rather than the roof, and that the term ‘roofed’ is misleading. The character and states were retained from Decker & Wozencraft (1991).

Distribution and polarity: State (0) is the ancestral condition for Procyonidae. State (1) occurs independently in *Urocyon cinereoargenteus* and at node 10.

27. Petrosal, floccular fossa: (0) present, deep; (1) absent or shallow, Figure 16 (Decker & Wozencraft, 1991).

The floccular fossa lies within the petrosal and opens medially to the endocranial cavity ventral to the anterior semicircular canal and dorsal to the common crus. The flocculus of the cerebellum is housed within the fossa (Evans, 1993). The floccular fossa is either large and deep, extending towards the lateral margin of the petrosal (state 0), or shallow to absent (state 1). As the difference between absent and shallow is ambiguous, these two conditions are combined into one state. The character and states were retained from Decker & Wozencraft (1991).

Distribution and polarity: The ancestral state for Procyonidae is a deep floccular fossa (state 0). The derived condition of a shallow floccular fossa (state 1) is present in *Mydaus javanensis* and at node 10.

28. Entotympanic inflation: (0) well inflated; (1) inflated; (2) reduced, Figure 17 (modified from Decker & Wozencraft, 1991).

The entotympanic is a separate ossification that partly forms the tympanic bulla and is often enlarged

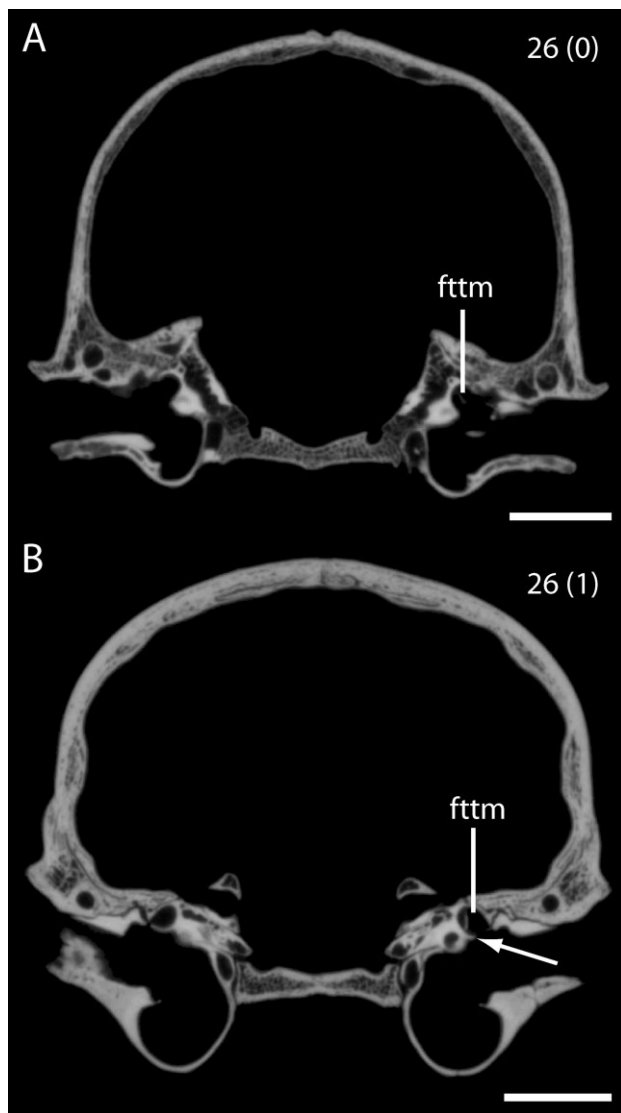


**Figure 15.** Character 26. Coronal slice, high-resolution X-ray computed tomography image. A, *Ailurus fulgens* ROM 180 slice 474; B, *Procyon lotor* TMM 778 slice 540. fttm, fossa for the tensor tympani muscle; white arrow: bony plate roofing the fossa. Scale bars = 1 cm.

in species with Type B bullae, such as *Procyon lotor* and *Nasua nasua* (Hunt, 1974). There are three states that describe the inflation of the entotympanic, including well inflated (state 0), inflated (state 1), and relatively uninflated, or reduced (state 2). The original character consisted of two states, including ‘well inflated’ and ‘reduced’ (Decker & Wozencraft, 1991). In my character, the ‘inflated’ state correlates to the ‘reduced’ state of Decker & Wozencraft (1991) and the ‘reduced’ state is exhibited by different taxa. The scoring of *Bassariscus astutus* was reinterpreted as ‘inflated’, which is consistent with Hunt’s (1974)

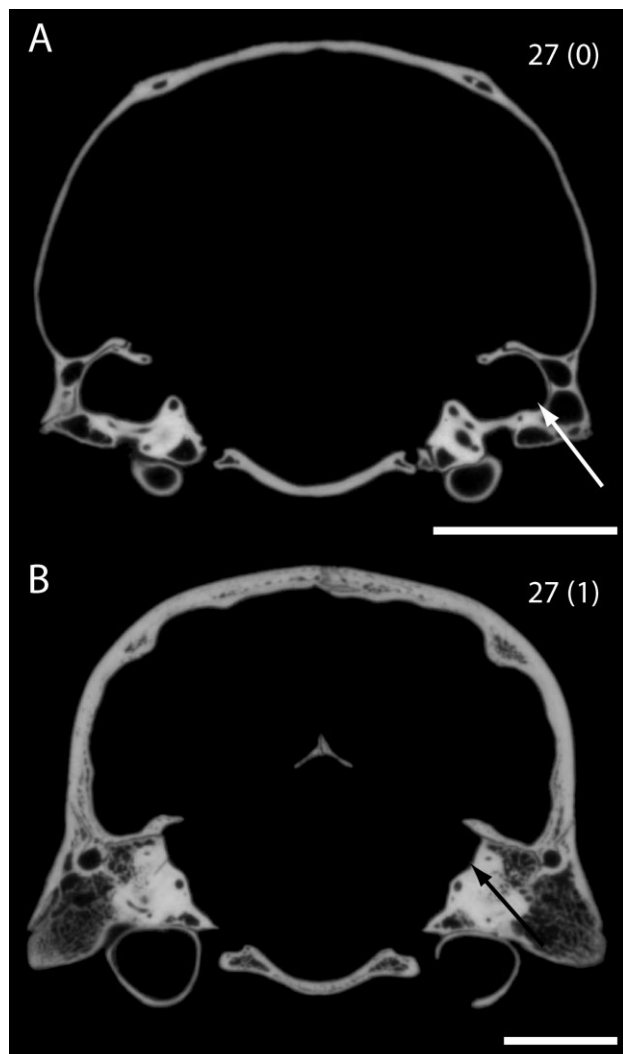


**Figure 16.** Character 27. Coronal slice, high-resolution X-ray computed tomography image. A, *Bassariscus astutus* TMM 473 slice 644; B, *Procyon lotor* TMM 778 slice 586. White and black arrows: location of the floccular fossa, if present. Scale bars = 1 cm.

interpretation that the caudal entotympanic is reduced and more primitive in *Bassariscus*.

**Distribution and polarity:** The primitive state for Procyonidae cannot be reconstructed. State (0) is present in *Urocyon cinereoargenteus*, *Martes pennanti*, and at node 10. State (1) is present independently in *Conepatus leuconotus*, *Bassariscus astutus*, and at node 9. State (2) is present independently in *Mydaus javanensis* and *Ailurus fulgens*.

29. Mastoid process, ventral extent: (0) dorsal to ventral border of meatal tube; (1) ventral to ventral border of meatal tube, Figure 18.

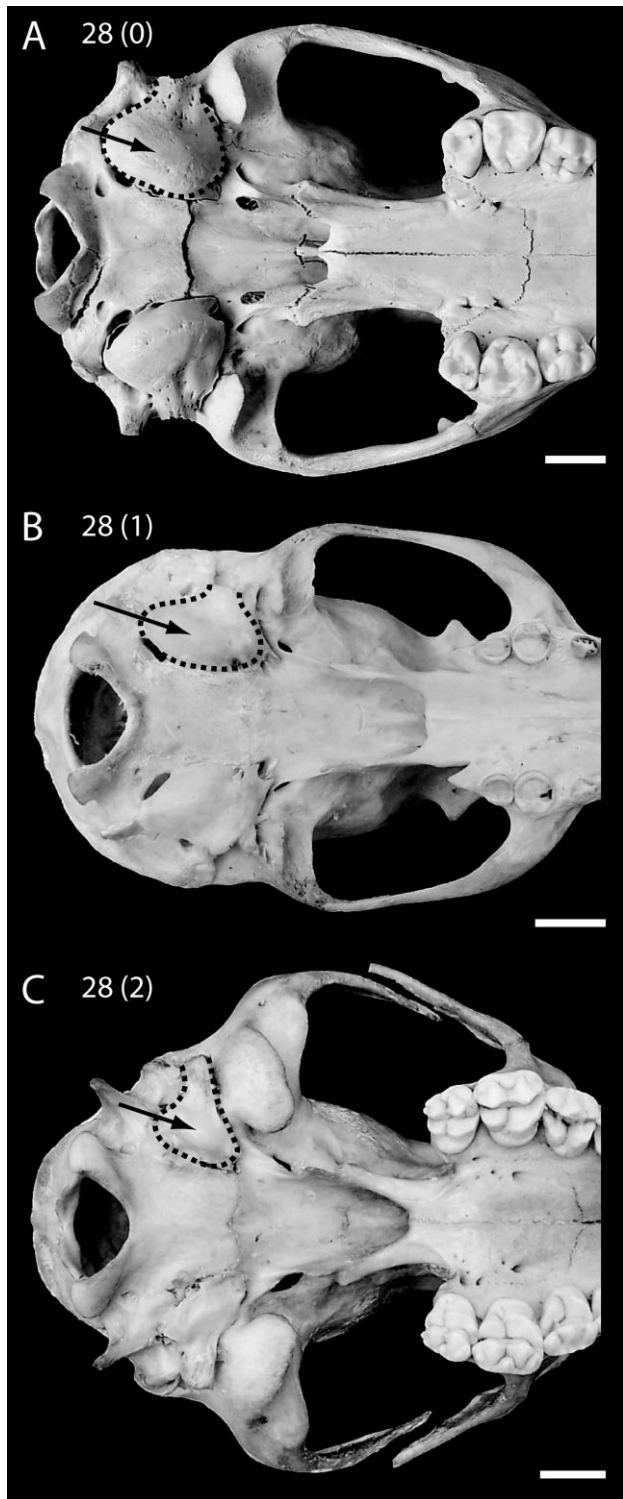


**Figure 17.** Character 28. Ventral view, anterior to the right. A, *Procyon lotor* TMM 778; B, *Potos flavus* MVZ 155212; C, *Ailurus fulgens* ROM 180. Black arrow: tympanic bulla. Scale bars = 1 cm.



**Figure 18.** Characters 29 and 30. Right lateral view, anterior to the right. A, *Bassariscus astutus* MVZ 192085; B, *Potos flavus* MVZ 132125; C, *Procyon lotor* TMM 778. Dashed black line: profile of mastoid process; solid black line: ventral margin of external auditory meatus. Scale bars = 1 cm.

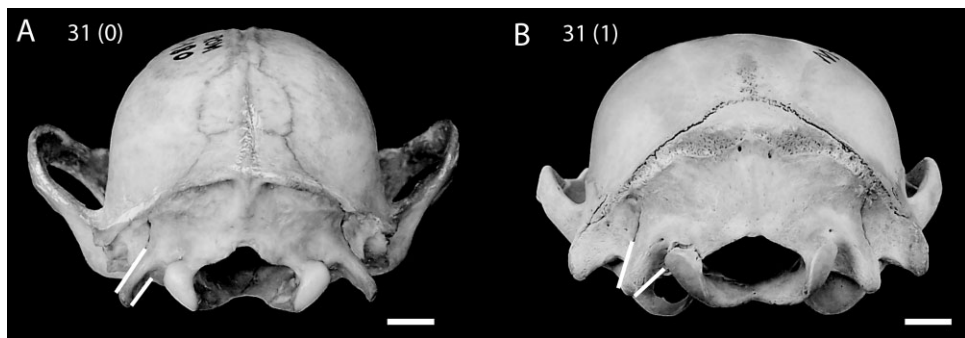


**Figure 19.** Character 31. Posterior view. A, *Ailurus fulgens* ROM 180; B, *Procyon lotor* TMM 778. Paired white lines: outline of paroccipital process. Scale bars = 1 cm.

The mastoid process, which serves as a muscle attachment site for the sternomastoideus muscle, extends to varying lengths posteriorly. The mastoid process either terminates dorsal to the ventral border of the meatal tube (state 0) or ventral to the ventral margin of the meatal tube (state 1). The position of the ventral margin of the mastoid process relative to the ventral border of the meatal tube in *Nasuella olivacea* was difficult to assess because of remaining soft tissue, and was thus scored as an uncertainty.

Distribution and polarity: State (0) is plesiomorphic for Procyonidae. State (1) is derived at node 10.

30. Mastoid process, lateral profile: (0) at a 45° angle; (1) horizontal; (2) vertical, Figure 18 (modified from Baskin, 2004: character 5).

The mastoid process of the petrosal exhibits different orientations in lateral view; the process either extends at a 45° angle posteroventrally (state 0), horizontal posteriorly (state 1), or vertically (state 1). The phrase ‘lateral profile’ was added to Baskin’s (2004) original character.

Distribution and polarity: State (0) is optimized as the ancestral condition for Procyonidae, and is present in *Urocyon cinereoargenteus*, at node 3, in *Bassariscus astutus*, and in *Nasuella olivacea*. State (1) is derived independently in *Martes pennanti* and at node 9. State (2) is present in *Ailurus fulgens*, *Procyon lotor*, and both species of *Nasua*; state (2) is optimized as derived at node 7.

31. Paroccipital process, posterior profile: (0) rectangular; (1) subtriangular, Figure 19.

The paroccipital process serves as the muscle attachment site for the digastric and jugulohyoid muscles and extends ventrally from the lateral aspect of the exoccipital. In posterior view, the process is either rectangular with a squared distal end (state 0) or subtriangular (state 1). The red panda, *Ailurus*

*fulgens*, has the most distinct paroccipital process morphology, with a relatively slender, columnar paroccipital process.

Distribution and polarity: State (0) is present in *Urocyon cinereoargenteus*, at node 3, and in *Ailurus fulgens*. State (1) is derived at node 4.

32. Rostrum, relative length: (0) intermediate; (1) elongate; (2) shortened, Figure 20 (modified from Baskin, 2004: character 8).

The rostrum, which is composed of the maxillae, premaxillae, and nasals, exhibits different relative lengths amongst the sampled taxa. The rostrum is either intermediate in length compared with the other two states (state 0), elongate, such that the rostrum makes up a greater proportion of the overall skull length (state 1), or shortened, such that it makes up a smaller proportion of the overall length of the skull (state 2). The character states and scoring of the taxa were consistent with Baskin (2004). However, the term ‘relative length’ was added in order to indicate that no discrete measurements delineate the different character states; additionally ‘normal’ was changed to ‘intermediate’.

Distribution and polarity: An intermediate rostrum length (state 0) is plesiomorphic for Procyonidae. State (1) is present independently in *Urocyon cinereoargenteus*, *Mydaus javanensis*, and at node 11. State (2) is derived independently in *Conepatus leuconotus*, *Ailurus fulgens*, and *Potos flavus*.

33. Angular process of dentary: (0) below level of tooth row; (1) above, Figure 21 (Baskin, 2004: character 10).

The angular process of the dentary is the smallest of the three processes of the ascending ramus and serves as the muscle attachment site of the medial pterygoid muscle medially and masseter muscle laterally. The apex of the angular process either lies in a plane ventral to the tooth row (state 0) or in a plane

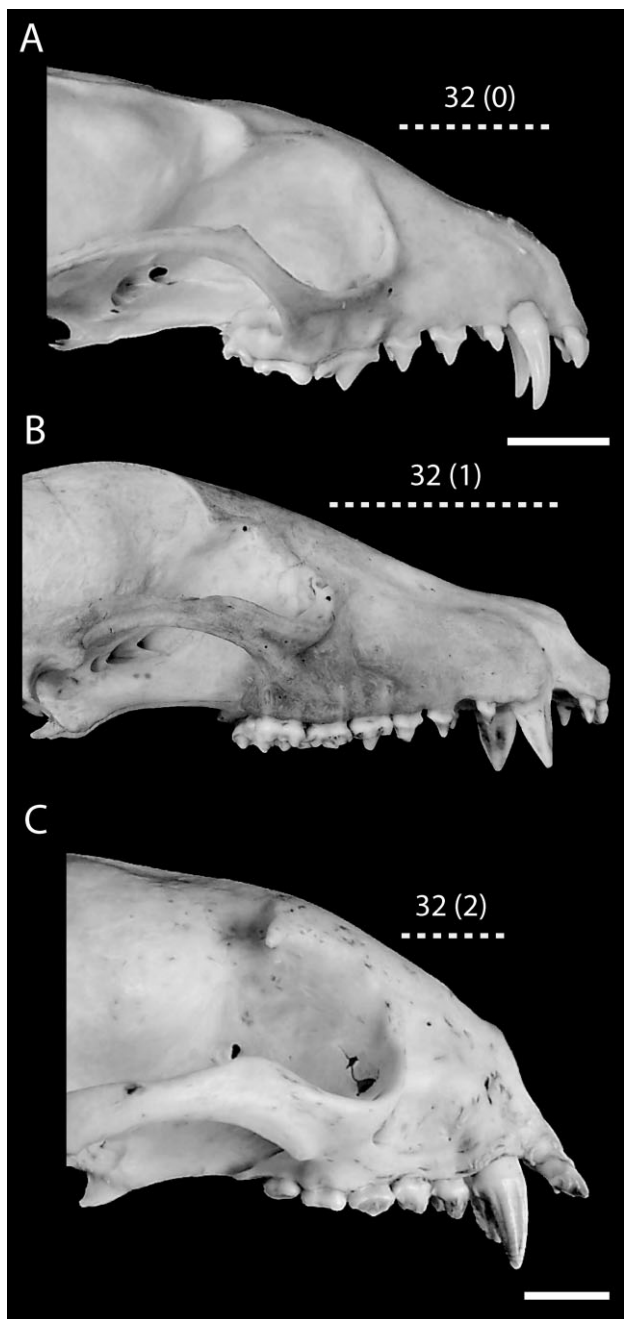


**Figure 20.** Character 32. Right lateral view, anterior to the right. A, *Bassariscus astutus* MVZ 192085; B, *Nasua narica* FMNH 14471; C, *Potos flavus* MVZ 132125. Dashed white line: rostrum length. Scale bars = 1 cm.

dorsal to the tooth row (state 1) when the dentary is positioned with the straightest portion in the horizontal plane. This character seems to correlate with flexion in the body of the dentary. If the dentary turns sharply dorsally at the posterior end, the angular process lies dorsal to the level of the tooth row. If the body of the dentary is generally straight or only

slightly bowed, the angular process lies ventral to the level of the tooth row. The state exhibited in the outgroup taxon, *Urocyon cinereoargenteus*, was difficult to score. The angular process occasionally lies in the same plane as the last molar; however, because the angular process usually lies below the level of the last molar in this species it was scored as possessing state (0). The condition in *Ailurus fulgens* is unknown because no dentaries were examined.

Distribution and polarity: State (0) is the primitive condition for Procyonidae, whereas state (1) is derived at node 10.

34. Angular process: (0) pronounced; (1) reduced, Figure 21 (modified from Decker & Wozencraft, 1991).

The angular process often is pronounced (state 0), but may be reduced in size (state 1). The reduced angular process is a relatively low projection on the posterior margin of the dentary, rather than a distinct process. In the original character, *Potos flavus* was scored as not possessing an angular process (Decker & Wozencraft, 1991). However, in the discussion of the autapomorphies of the kinkajou, a reduced angular process was included (Decker & Wozencraft, 1991). The angular process is indeed reduced, rather than absent, in *Potos flavus*.

Distribution and polarity: State (0) is the ancestral condition for Procyonidae, and state (1) is an autapomorphy of *Potos flavus*.

35. Mandibular symphysis: (0) weak; (1) strongly fused, Figure 21 (Decker & Wozencraft, 1991).

The mandibular symphysis is either weak and unfused (state 0) or strongly fused (state 1). The character states and scorings were congruent with Decker & Wozencraft (1991).

Distribution and polarity: State (0) is the plesiomorphic condition for Procyonidae, whereas state (1) is derived independently in *Mydaus javanensis* and *Potos flavus*. The inclusion of *Mydaus javanensis* indicates that state (1) is a local autapomorphy within Procyonidae, rather than an autapomorphy as in Decker & Wozencraft (1991).

#### DENTAL CHARACTERS

36. Upper incisor 3: (0) larger than I1 and I2; (1) equal to I1 and I2, Figure 22 (Decker & Wozencraft, 1991).

The third upper incisor is either larger than the first two incisors (state 0) or equal in size to I1 and I2 (state 1). My character scoring was consistent with that of Decker & Wozencraft (1991).

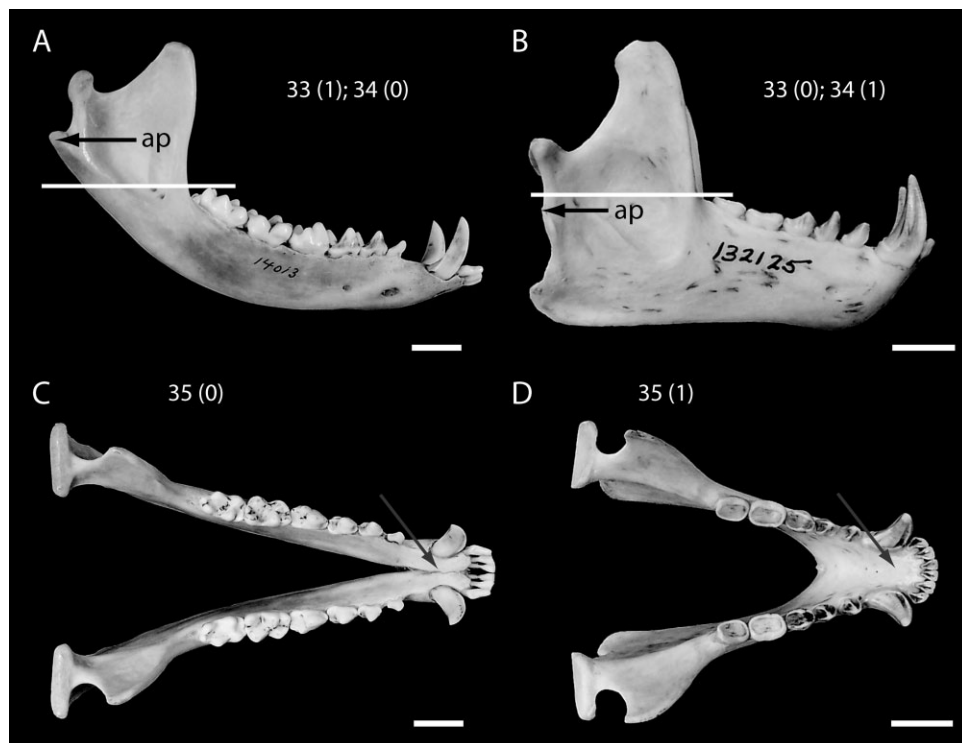


**Figure 21.** Characters 33, 34, and 35. A, B, right lateral view; C, D, dorsal view, anterior to the right. A, C, *Nasua narica* FMNH 14013; B, D, *Potos flavus* MVZ 132125. White line: level of tooth row; ap, angular process; grey arrow: location of mandibular symphysis, if present. Scale bars = 1 cm.

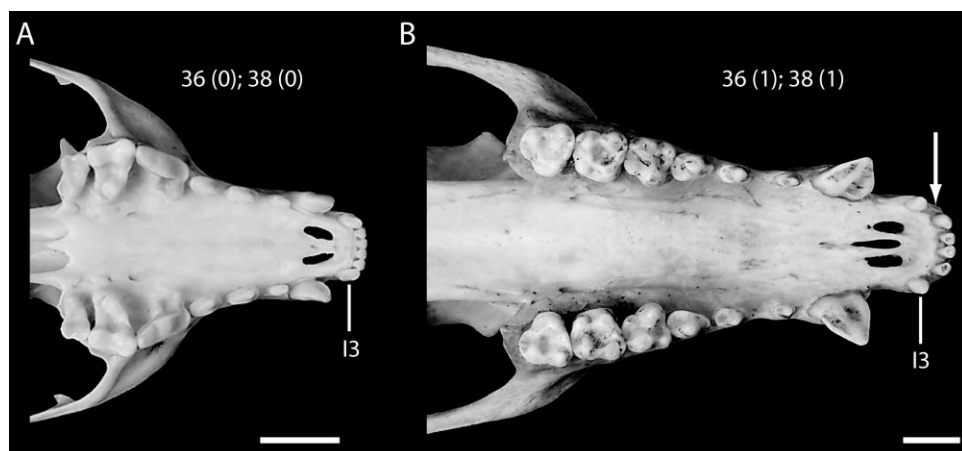


**Figure 22.** Characters 36 and 38. Ventral view, anterior to the right. A, *Bassariscus astutus* MVZ 192085; B, *Nasua narica* FMNH 14471. I3, third incisor; white arrow: diastema. Scale bars = 1 cm.

Distribution and polarity: State (0) is the primitive condition and state (1) is derived for node 3 and node 11. This character is a synapomorphy of the coatimundis.

37. Lower incisors: (0) vertical; (1) procumbent, Figure 23 (Decker & Wozencraft, 1991).

The lower incisors may be vertically orientated (state 0) or procumbent (state 1), such that they project anteriorly. The character and character states were retained from Decker & Wozencraft (1991).

Distribution and polarity: The ancestral condition for Procyonidae is state (0). State (1) is present

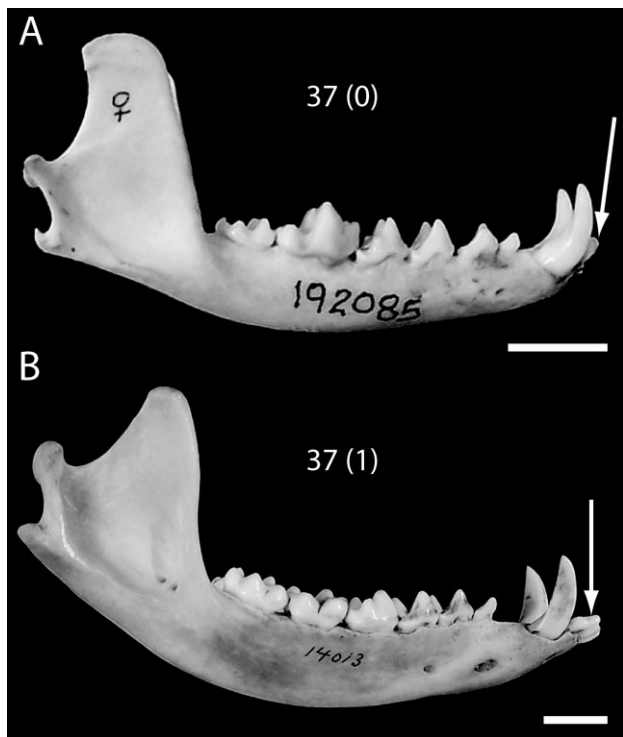


**Figure 23.** Character 37. Right lateral view, anterior to the right. A, *Bassariscus astutus* MVZ 192085; B, *Nasua narica* FMNH 14013. White arrow: lower incisors. Scale bars = 1 cm.

independently in *Urocyon cinereoargenteus*, *Mydaus javanensis*, and at node 11.

38. Diastema between I<sub>2</sub> and I<sub>3</sub>: (0) absent; (1) present, Figure 22 (Decker & Wozencraft, 1991).

A diastema may be present (state 1) between the second and third upper incisors, which is not larger than the width of the second incisor. The character and character states were retained from Decker & Wozencraft (1991).

Distribution and polarity: State (0) is the ancestral condition for Procyonidae. State (1) is derived independently in *Urocyon cinereoargenteus* and at node 11.

39. Canine, buccal surface: (0) ungrooved; (1) narrow grooves; (2) broad grooves, Figure 24.

Both the upper and lower canines may possess grooves on the buccal surface. Narrow grooves (state 1) are often two in number, but may deviate from that number. Broad grooves (state 2) are also generally two in number on the upper canines; however, only one groove is generally present on the lower canine, such that the buccal surface of the lower canine is fairly flat. Canine grooves in members of the Potosi-

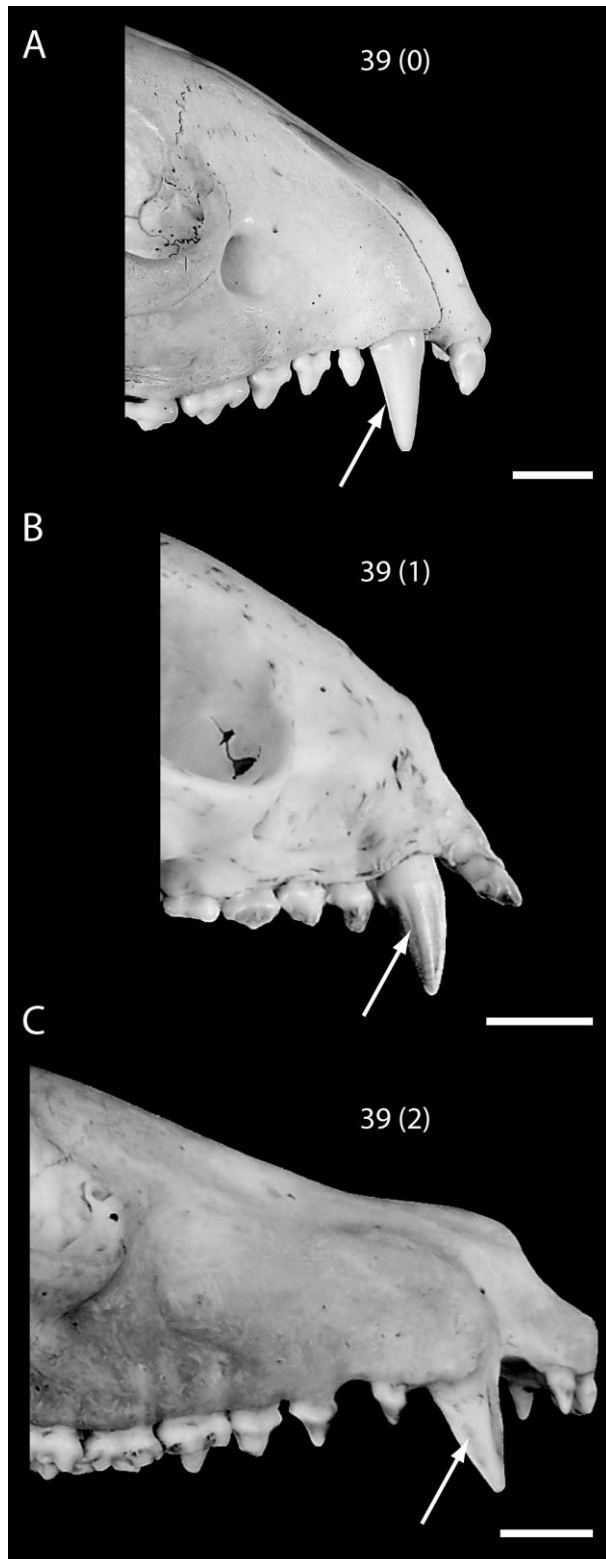


**Figure 24.** Character 39. Right lateral view, anterior to the right. A, *Procyon lotor* TMM 778; B, *Potos flavus* MVZ 132125; C, *Nasua narica* FMNH 14471. White arrow: location of canine grooves, if present. Scale bars = 1 cm.

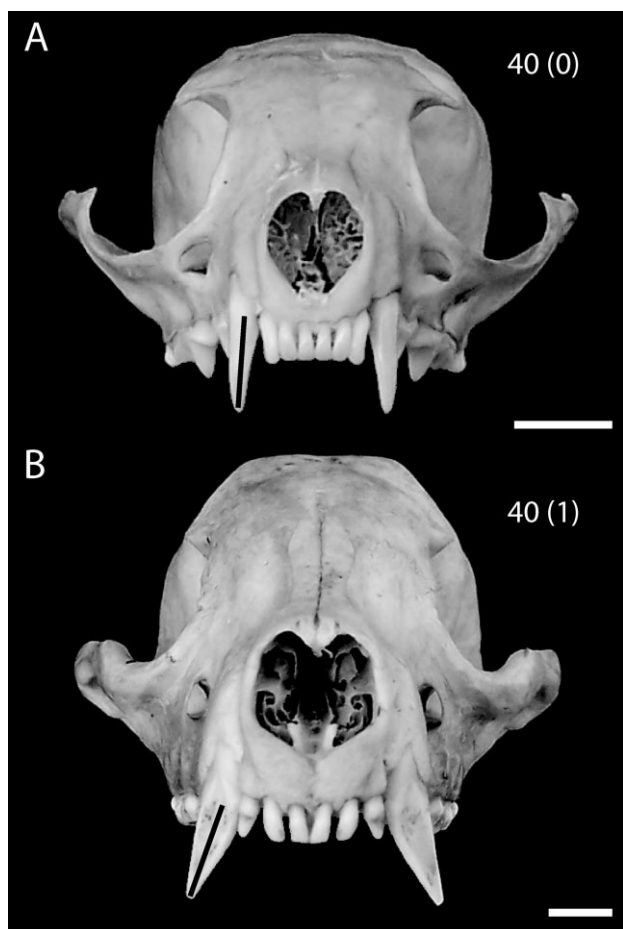


**Figure 25.** Character 40. Anterior view. A, *Bassariscus astutus* MVZ 192085; B, *Nasua narica* FMNH 14471. Black line: orientation of upper canine. Scale bars = 1 cm.

nae have been discussed (Decker & Wozencraft, 1991), but have not been included in any previous phylogenetic analysis.

Distribution and polarity: State (0) is the plesiomorphic state for Procyonidae. State (1) is derived at node 8. State (2) is derived for node 11.

40. Upper canines: (0) directed ventrally; (1) flared laterally, Figure 25 (Decker & Wozencraft, 1991).

The upper canines are either directed ventrally (state 0) or flared laterally (state 1). The character and states were retained from Decker & Wozencraft (1991).

Distribution and polarity: State (0) is the ancestral condition for Procyonidae. State (1) is derived for node 11; this character is a synapomorphy of the coati mundis.

41. Diastema between C and P1/P2: (0) absent; (1) present, Figure 26 (modified from Decker & Wozencraft, 1991).

A diastema may be present (state 1) between the crowns of the upper canine (C) and first or second premolar (P1 or P2), and is no smaller than the anteroposterior length of the first premolar. The presence of a diastema between C and P1/P2 may correlate with an elongated rostrum, much like the diastema between the second and third upper incisors. The character was emended from Decker & Wozencraft (1991) to include 'P2' for taxa that do not have a first upper premolar.

Distribution and polarity: State (0) is the ancestral condition for Procyonidae. State (1) is present independently in *Urocyon cinereoargenteus*, *Mydaus javanensis*, and at node 11.

42. P1/p1: (0) single rooted; (1) tooth reduced to absent; (2) double rooted, Figure 26 (modified from Baskin, 2004: character 11).

The first upper and lower premolars either have one root (state 0) or two roots (state 2), or may be entirely absent (state 1). The character and character states were retained from Baskin (2004), with only the addition of the word 'tooth' to state (1). The condition of having reduced P1 and p1 was not observed in any sampled taxa.

Distribution and polarity: State (0) is the primitive condition for Procyonidae. State (1) is independently derived at node 3, in *Ailurus fulgens*, and in *Potos flavus*. State (2) is derived for node 11; the condition is a synapomorphy of the coati mundis.

43. P3/p2–3: (0) slender; (1) anteroposteriorly compressed/transversely broadened, Figure 26 (Baskin, 2004: character 12).

The upper third premolar and lower second and third premolars may be slender (state 0), such that they are relatively the same width for the entire length of the tooth. Alternatively, the premolars may be anteroposteriorly compressed and transversely broadened (state 1) towards the distal end of the tooth. The character was retained from Baskin (2004), but the scoring was altered. Under the original scoring *Nasua* and *Edaphocyon pointblankensis* were scored as exhibiting state 0; however, those premolars are in fact transversely broadened (state 1).

Distribution and polarity: State (0) is the plesiomorphic state for Procyonidae, and present independently in *Nasuella olivacea*. State (1) is derived at node 6 and lost in *Nasuella olivacea*.

44. P3: (0) one or two roots; (1) three roots, Figure 26 (Decker & Wozencraft, 1991).

The third upper premolar either has one or two roots (state 0) or three roots (state 1). The character and character states were retained from Decker & Wozencraft (1991).

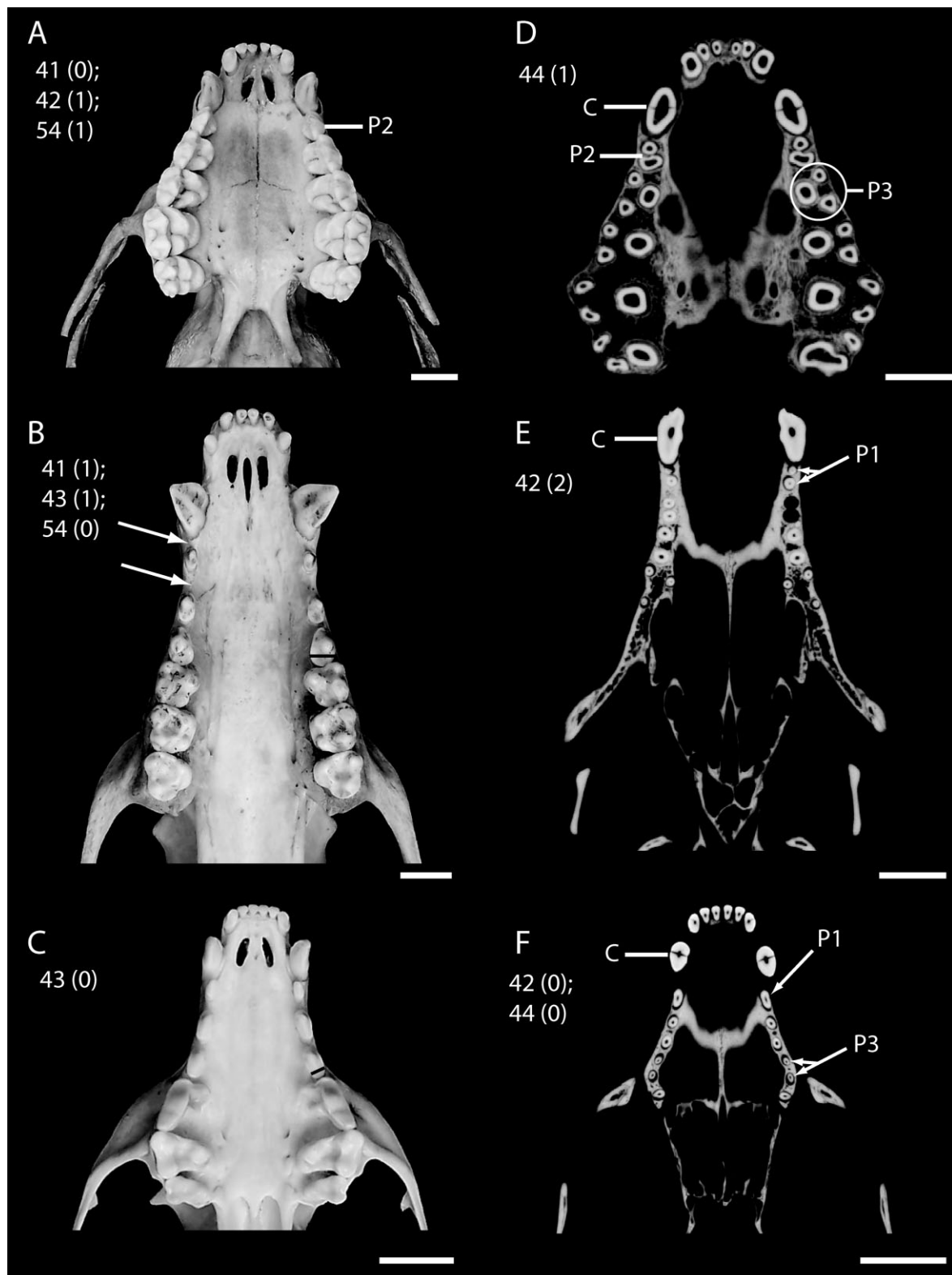


**Figure 26.** Characters 41, 42, 43, 44, and 54. A–C, ventral view; D–F, horizontal plane, anterior directed upwards. A, D, *Ailurus fulgens* ROM 180 slice 536; B, *Nasua narica* FMNH 14471; C, *Bassariscus astutus* MVZ 192085; E, *Nasua narica* FMNH 14013 slice 403; F, *Bassariscus astutus* TMM 473 slice 368. White arrow: diastema; black line: premolar width; P1, first premolar; P2, second premolar; P3, third premolar; C, canine. Scale bars = 1 cm.

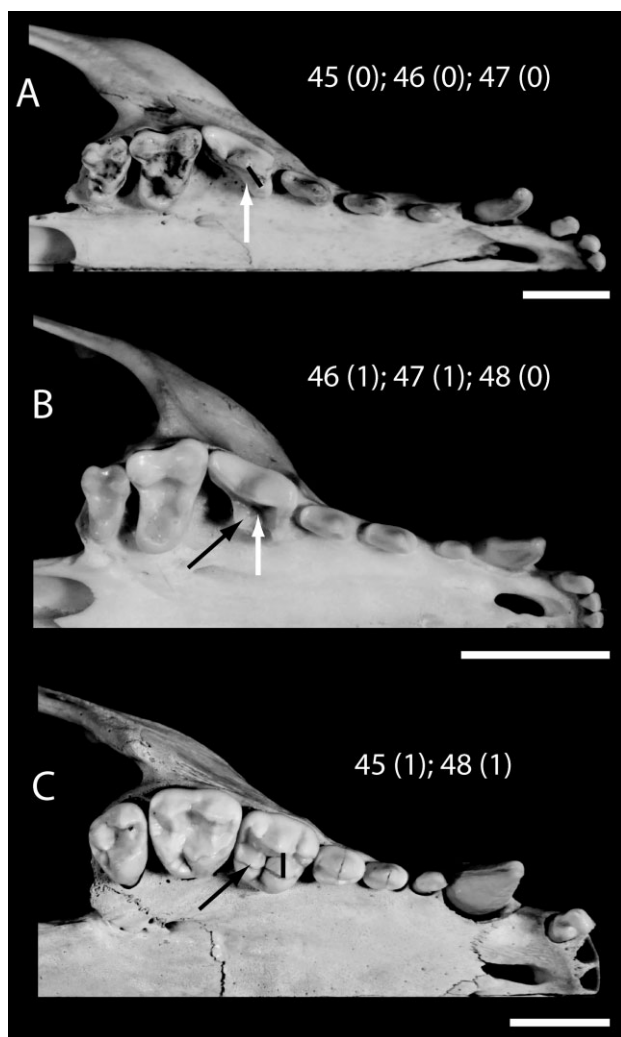


**Figure 27.** Characters 45, 46, 47, and 48. Right dentition in ventral view, anterior to the right. A, *Urocyon cinereoargenteus* MVZ 114285; B, *Bassariscus astutus* MVZ 192085; C, *Procyon lotor* TMM 778. Black line: protocone-paracone positional relationship; white arrow: internal shelf; black arrow: hypocone. Scale bars = 1 cm.

Distribution and polarity: State (0) is the ancestral condition for Procyonidae. State (1) is derived independently in *Ailurus fulgens* and *Potos flavus*.

45. P4 protocone: (0) anteromedial to paracone; (1) directly medial to paracone, Figure 27 (modified from Baskin, 2004: character 14).

The protocone of the fourth upper premolar is either located anteromedial to (state 0) or directly medial to (state 1) the paracone. The protocone may also be posteromedial to the paracone and was scored as state (1). This character was modified from the original, in which the intermediate state ‘not as anterior’ was removed because it was difficult determine

‘not as anterior’ versus ‘anterior’. Additionally, a reference point (the paracone) and ‘directly’ were added for specificity.

Distribution and polarity: The primitive condition for Procyonidae is state (0), which is also present in *Ailurus fulgens*. State (1) is derived at node 3 and node 6.

46. P4 internal shelf: (0) weakly developed; (1) present, Figure 27 (Baskin, 2004: character 15).

A shelf on the medial side of the fourth upper premolar is either so weakly developed that it is effectively absent (state 0) or present (state 1). The character and character states were retained from Baskin (2004).

Distribution and polarity: State (0) is the primitive musteloid condition. State (1) is derived in *Mydaus javanensis* and at node 5, Procyonidae.

47. P4 hypocone: (0) absent; (1) present, Figure 27 (Decker & Wozencraft, 1991; modified from Baskin, 2004: character 16).

The hypocone of the fourth upper premolar is either absent (state 0) or present (state 1). When present, the cusp is positioned posterior to the protocone. The character and character states were retained from Decker & Wozencraft (1991); however, Baskin’s (2004) version of the character included additional states that referred to the size of the hypocone. Those states were included here as a separate character. In the original scoring, *Bassariscus* was scored as possessing state (0), because more plesiomorphic species of *Bassariscus* do not have a hypocone (Baskin, 2004). As I only scored *Bassariscus astutus*, which exhibits state (1), *Bassariscus* was scored for the presence of a hypocone on P4.

Distribution and polarity: State (0) is reconstructed as ancestral at the base of the tree. State (1) is derived at node 5, Procyonidae. The hypocone is then lost at node 9, which includes *Bassaricyon alleni* and *Potos flavus*.

48. P4 hypocone size: (0) small; (1) large, Figure 27 (modified from Baskin, 2004: character 16).

When present, the hypocone is either small (state 0) or large (state 1). This character was originally incorporated with the previous character in Baskin’s (2004) analysis of procyonid relationships.

Distribution and polarity: State (0) is the primitive condition, and is present in *Bassariscus astutus* and *Edaphocyon pointblankensis*. State (1) is derived at node 7.

49. P4 metacone blade: (0) present; (1) absent, Figure 28 (modified from Baskin, 2004: character 17).

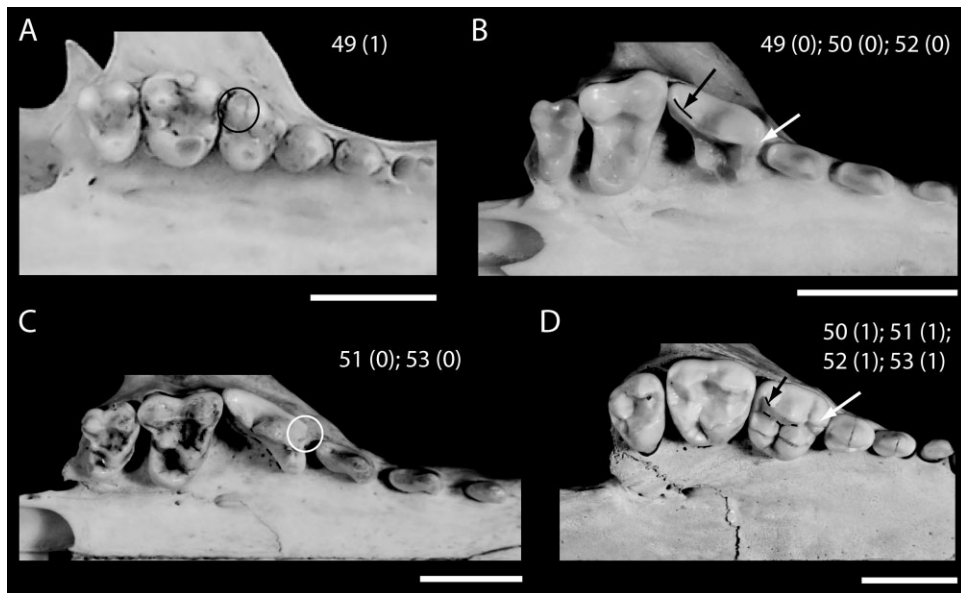


**Figure 28.** Characters 49, 50, 51, 52, and 53. Right dentition in ventral view, anterior to the right. A, *Bassaricyon alleni* FMNH 41502; B, *Bassariscus astutus* MVZ 192085; C, *Urocyon cinereoargenteus* MVZ 114285; D, *Procyon lotor* TMM 778. Black circle: absence of metacone blade; black arrow and black line: length of metacone blade; white circle: absence of parastyle; white arrow: parastyle; dashed black line: carnassial shear. Scale bars = 1 cm.

The metacone blade, a ridge extending distally from the metacone, on the fourth upper premolar is either present (state 0) or absent (state 1). The original character included additional states that referred to the elongation of the metacone blade (Baskin, 2004); these states were included here as a separate character.

Distribution and polarity: State (0) is the plesiomorphic state for Procyonidae. State (1) is derived at node 9, and is a synapomorphy of *Bassaricyon alleni* plus *Potos flavus*.

50. P4 metacone blade: (0) elongate; (1) reduced, Figure 28 (modified from Baskin, 2004: character 17).

The metacone blade can vary in length, from elongate (state 0) to reduced (state 1). This character was originally incorporated with the previous character (Baskin, 2004). I modified the character states such that the intermediate state ‘not as reduced’ was removed, because it was difficult to distinguish ‘not as reduced’ from ‘reduced’. Additionally, the scoring of *Bassariscus astutus* was changed from that of Baskin (2004) as the metacone blade shares the same morphology as *Urocyon cinereoargenteus* and *Martes pennanti*.

Distribution and polarity: State (0) is the ancestral condition for Procyonidae. State (1) is independently derived in *Mydaus javanensis* and at node 6.

51. P4 parastyle: (0) absent; (1) present, Figure 28 (Decker & Wozencraft, 1991; modified from Baskin, 2004: character 18).

On the fourth upper premolar a parastyle, which is positioned mesial to the paracone, is either absent (state 0) or present (state 1). The character and character states were retained from Decker & Wozencraft (1991); however, Baskin’s (2004) version of the character included additional states that referred to the size of the parastyle. These states were included here as a separate character.

Distribution and polarity: The parastyle is present in all taxa except *Urocyon cinereoargenteus* and *Conepatus leuconotus*. State (1) is plesiomorphic for Procyonidae, node 5.

52. P4 parastyle size: (0) small; (1) enlarged, Figure 28 (modified from Baskin, 2004: character 18).

The parastyle exhibits different sizes, from small (state 0) to enlarged (state 1). This character was originally incorporated with the previous character (Baskin, 2004) and was modified, such that the state ‘greatly enlarged’ was removed because no taxon exhibited that condition. The extant *Bassariscus astutus* was rescored as possessing a small parastyle.

Distribution and polarity: State (0) is the primitive condition for Procyonidae. State (1) is derived at node 6, and is lost at node 9.

53. Carnassial shear on P4: (0) sectorial; (1) nonsectorial, Figure 28 (modified from Decker & Wozencraft, 1991).

The carnassial shear on the fourth upper premolar was described by Decker & Wozencraft (1991) as either trenchant (state 0) or rounded (state 1). The meaning of ‘trenchant’ versus ‘rounded’ carnassial shear is unclear; thus, the states were scored as sectorial versus nonsectorial, respectively. The character states were changed accordingly.

**Distribution and polarity:** State (0) is the ancestral condition and is present in *Urocyon cinereoargenteus*, node 3, *Martes pennanti*, and *Bassariscus astutus*. State (1) is derived at node 6.

54. Diastema between P1 and P2: (0) present; (1) absent, Figure 26 (Decker & Wozencraft, 1991).

A diastema may be present (state 0) between the first and second upper premolars. The presence of a diastema between P1 and P2 may be correlated with an elongated rostrum; however, the diastema is also present in *Bassariscus astutus*, which does not have an elongated rostrum. The character and character states were retained from Decker & Wozencraft (1991). *Bassariscus astutus* was rescored in this analysis because there is a diastema present between the first two premolars.

**Distribution and polarity:** The ancestral condition cannot be reconstructed at the base of the tree. State (0) is present in *Urocyon cinereoargenteus*, *Bassariscus astutus*, *Edaphocyon pointblankensis*, and at node 11. State (1) is present at node 3, in *Martes pennanti*, at node 8, and in *Procyon lotor*.

55. Upper molars: (0) triangular with distinct cusps; (1) rounded with reduced cusps, Figure 29 (Baskin, 2004: character 19).

The upper molars are either triangular with distinct cusps (state 0) or more rounded with reduced cusps (state 1). *Martes pennanti* possesses a somewhat ambiguous condition because the presence of an expanded posterointernal cingulum gives the molar a more rectangular shape. However, the overall morphology is more like that of *Urocyon cinereoargenteus* and *Bassariscus astutus* than *Procyon lotor*. Thus, *Martes pennanti* was scored as possessing state (0). The character and character states were retained from Baskin (2004).

**Distribution and polarity:** State (0) is the ancestral condition for Procyonidae. State (1) is derived in *Conepatus leuconotus* and at node 7.

56. Upper molars with external cingulum: (0) present; (1) reduced to absent, Figure 29 (Baskin, 2004: character 20).



**Figure 29.** Characters 55, 56, and 64. Right dentition in ventral view, anterior to the right. A, *Urocyon cinereoargenteus* MVZ 11428; B, *Procyon lotor* TMM 778. Black arrow: external cingulum; black line: paracone–metacone positional relationship. Scale bars = 1 cm.

The upper molars may possess a distinct external cingulum (state 0), a shelf-like ledge, or the cingulum may be reduced in size to absent (state 1). The condition exhibited by *Potos flavus* is somewhat ambiguous because the cusps are so reduced that identification of a cingulum can be difficult. The character and character states were retained from Baskin (2004).

**Distribution and polarity:** State (0) is the primitive condition for Procyonidae. State (1) is independently derived in *Mydaus javanensis* and at node 10.

57. M1 parastyle: (0) enlarged; (1) small, Figure 30 (modified from Baskin, 2004: character 21).

The parastyle on the upper first molar is either enlarged (state 0) or small (state 1). The character was retained from Baskin (2004), but the character states were reversed. *Potos flavus* was rescored as having a small parastyle to indicate that it shares the same condition of the first upper molar parastyle as *Bassaricyon alleni*.

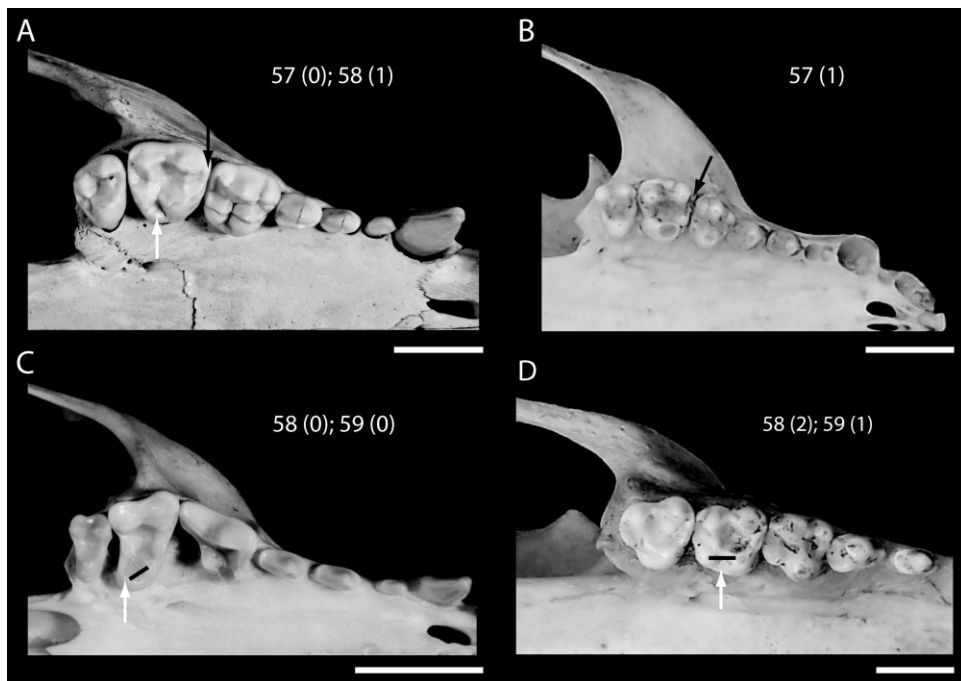


**Figure 30.** Characters 57, 58, and 59. Right dentition in ventral view, anterior to the right. A, *Procyon lotor* TMM 778; B, *Bassaricyon alleni* FMNH 41502; C, *Bassariscus astutus* MVZ 192085; D, *Nasua narica* FMNH 14471. Black arrow: parastyle; white arrow: hypocone; black line: hypocone–protocone positional relationship. Scale bars = 1 cm.

Distribution and polarity: State (0) is the ancestral condition for Procyonidae. State (1) is derived at node 9, and is a synapomorphy of *Bassaricyon alleni* plus *Potos flavus*.

58. M1 hypocone: (0) present; (1) reduced; (2) greatly reduced to absent, Figure 30 (Baskin, 2004: character 22).

The hypocone on the first upper molar is either present (state 0), reduced in size (state 1), or greatly reduced in size to absent (state 2). State (2) was not divided into separate states because the hypocone may be so small that it is unclear whether the cusp is present or not, such as in *Nasua*. The character and character states were retained from Baskin (2004).

Distribution and polarity: State (0) is plesiomorphic for Procyonidae, and exhibited in *Urocyon cinereoargenteus*, *Bassariscus astutus*, and *Edaphocyon point-blankensis*. State (1) is present at node 3 and in *Procyon lotor*. State (2) is present in *Martes pennanti* and at node 7.

59. M1 hypocone (or internal cingulum if hypocone is absent): (0) posterointernal to protocone; (1) posterior to protocone, Figure 30 (modified from Baskin, 2004: character 23).

The hypocone (or internal cingulum) on the upper first molar is generally positioned posterointernally to

the protocone (state 0), or may be posterior to the protocone (state 1). As no sampled taxa possessed a hypocone (or internal cingulum) internal to the protocone, the character state ‘interior’ of Baskin (2004) was excluded. Additionally, the character state ‘expanded posterointernally’ was changed to ‘posterointernal to protocone’ because there is no variation amongst taxa in the degree of posterointernal expansion of the hypocone. As *Potos flavus* has molars without defined cusps or cingula, this taxon was scored as inapplicable.

Distribution and polarity: State (0) is the plesiomorphic state for Procyonidae. State (1) is derived at node 11.

60. M1 metaconule: (0) present; (1) absent, Figure 31 (modified from Baskin, 2004: character 24).

The metaconule of the first upper molar is either present (state 0) or absent (state 1). The character and character states were modified from Baskin’s (2004) analysis in which the character included additional states referring to the size of the metaconule. These states were included in a separate character. Additionally, the character ‘secondarily reduced to absent’ (Baskin, 2004) was excluded, because it requires an a priori assumption of the evolution of the character. *Bassaricyon alleni* was rescored to indicate the presence of a metaconule. There may be identity

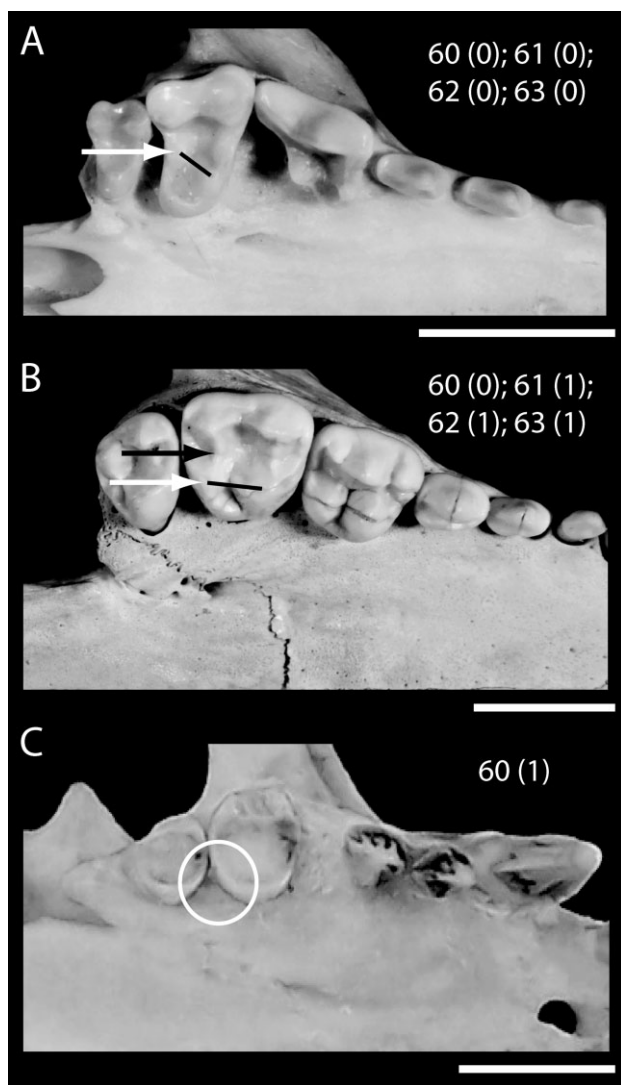


**Figure 31.** Characters 60, 61, 62, and 63. Right dentition in ventral view, anterior to the right. A, *Bassariscus astutus* MVZ 192085; B, *Procyon lotor* TMM 778; C, *Potos flavus* MVZ 155212. White arrow: metaconule; white circle: absence of metaconule; black line: metaconule-protocone positional relationship; black arrow: crest. Scale bars = 1 cm.

issues with the M1 metaconule because Decker & Wozencraft (1991) believed the cusp is actually homologous to the hypocone rather than the metaconule.

Distribution and polarity: State (0) is present in *Urocyon cinereoargenteus* and at node 5, Procyonidae. State (1) is present at node 3, in *Martes pennanti*, and in *Potos flavus*.

61. M1 metaconule: (0) small; (1) prominent, Figure 31 (modified from Baskin, 2004: character 24).

The metaconule can exhibit different sizes, from small (state 0) to prominent (state 1). The character was originally incorporated with the previous character (Baskin, 2004). The character states were modified here, such that the state ‘present’ was replaced with ‘small’.

Distribution and polarity: State (0) is the plesiomorphic state for Procyonidae and present in *Bassaricyon alleni*. State (1) is present in *Ailurus fulgens* and at node 10; the condition at node 7 cannot be reconstructed.

62. M1 metaconule position: (0) posteroexternal to protocone; (1) posterior to protocone, Figure 31 (Baskin, 2004: character 25).

The metaconule is positioned either posteroexternal to the protocone (state 0) or posterior to the protocone (state 1). The character and character states were retained from Baskin (2004).

Distribution and polarity: State (0) is the ancestral condition for Procyonidae, whereas state (1) is derived at node 10.

63. M1 metacone: (0) not connected to metaconule; (1) connected by crest, Figure 31 (Baskin, 2004: character 26).

The metaconule, when present, is either separate from the metacone (state 0) or connected by a crest (state 1). The character and character states were retained from Baskin (2004).

Distribution and polarity: State (0) is the primitive condition for Procyonidae. State (1) is derived in *Edaphocyon pointblankensis* and at node 10.

64. M2 paracone and metacone: (0) close together; (1) separated, Figure 29 (Baskin, 2004: character 27).

The paracone and metacone of the second upper molar are either close together (state 0) or separated (state 1), such that they are not connected. The character and character states were retained from Baskin (2004). The character could not be scored for *Martes pennanti*, *Mydaus javanensis*, and *Conepatus leuconotus* because these taxa lack a second upper molar.

Distribution and polarity: State (0) is present only in *Urocyon cinereoargenteus*. State (1) is derived at node 5, Procyonidae.

65. m1 trigonid: (0) paracristid blade-like, with paraconid anteriorly placed; (1) paraconid and metaconid close together; (2) with paraconid, protoconid, and metaconid more or less equally spaced, Figure 32 (modified from Baskin, 2004: character 28).

The trigonid of the lower first molar can exhibit different spatial relationships of the cusps, including

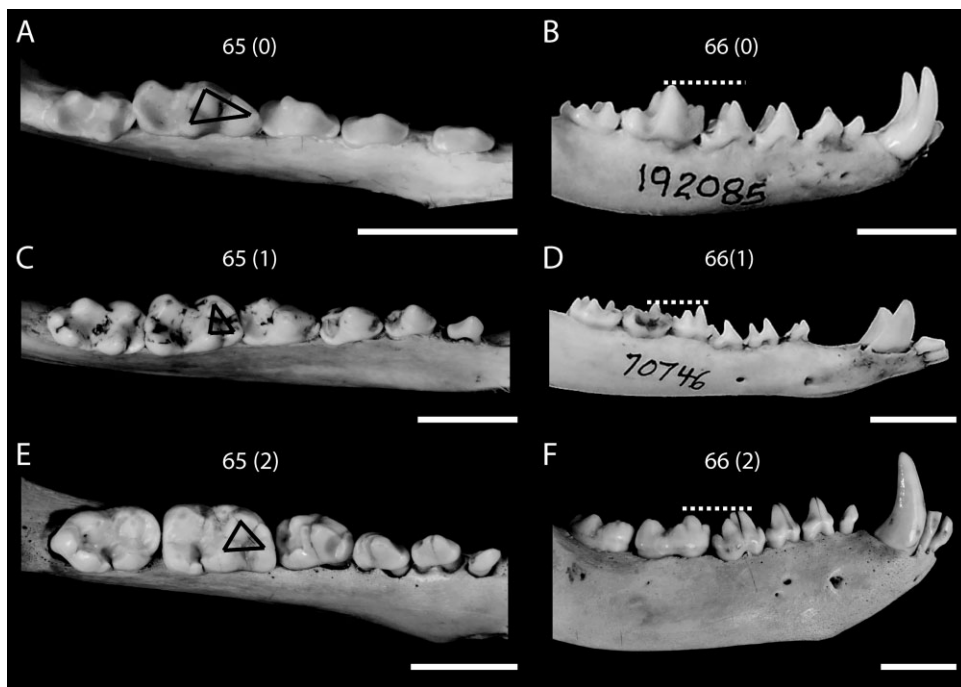


**Figure 32.** Characters 65 and 66. A, C, E, left dentition in dorsal view; B, D, E, right dentition in lateral view, anterior to the right. A, B, *Bassariscus astutus* MVZ 192085; C, *Nasua narica* FMNH 14013; D, *Nasuella olivacea* FMNH 70746; E, F, *Procyon lotor* TMM 778. Black triangle: paraconid–metacanid–protoconid positional relationships; dashed white line: protoconid–fourth premolar proportional height. Scale bars = 1 cm.

having the paracristid blade-like and paraconid anteriorly placed (state 0), the paraconid and metacanid close together (state 1), or with the paraconid, protoconid, and metacanid more or less equally spaced (state 2). State (2) of the original character ‘paraconid and metacanid adjacent’ (Baskin, 2004) was eliminated, because the difference between ‘close together’ of state (1) and ‘adjacent’ of state (2) was ambiguous. Character states (0) and (3) of Baskin (2004) were reversed. Additionally, ‘paraconid’ of the original state 3 was changed to ‘paracristid’ because it is the paracristid, rather than the paraconid, that is blade-like. My interpretation of this character led to almost complete rescored of all extant taxa. *Bassariscus astutus* was scored as having an anteriorly placed, blade-like paraconid (state 0). *Procyon lotor* was rescored as exhibiting state (2) because the three cusps are more equally spaced in the raccoon, with the protoconid and metacanid being slightly closer to one another. *Ailurus fulgens* could not be scored for this character, because no dentaries were examined.

Distribution and polarity: State (0) is the primitive condition for Procyonidae. State (1) is derived at node 7. State (2) is derived only in *Procyon lotor*, and thus an autapomorphy of that taxon.

66. m1 protoconid: (0) taller than p4; (1) equal to p4; (2) lower than p4, Figure 32 (modified Baskin, 2004: character 29).

The protoconid of the first lower molar is either taller than the cusps on the fourth premolar (state 0), equal in height to the p4 (state 1), or lower than the p4 (state 2). The character states were slightly modified from Baskin (2004) to include the reference point of ‘p4’ in states (1) and (2) in addition to state (0).

Distribution and polarity: State (0) is reconstructed as ancestral for Procyonidae, and is exhibited by *Urocyon cinereoargenteus*, *Mydaus javanensis*, *Martes pennanti*, and *Bassariscus astutus*. State (1) is present only in *Nasuella olivacea*, and thus an autapomorphy of the taxon. State (2) is derived at node 7.

67. m1 paraconid: (0) present; (1) absent, Figure 33 (modified from Baskin, 2004: character 31).

The paraconid on the first lower molar is either present (state 0) or absent (state 1). Additional states referring to the size of the paraconid were originally included in Baskin’s (2004) analysis; here, these states were included in a separate character.

Distribution and polarity: State (0) is plesiomorphic for Procyonidae. State (1) is derived only in *Potos flavus*, and thus an autapomorphy of that taxon.

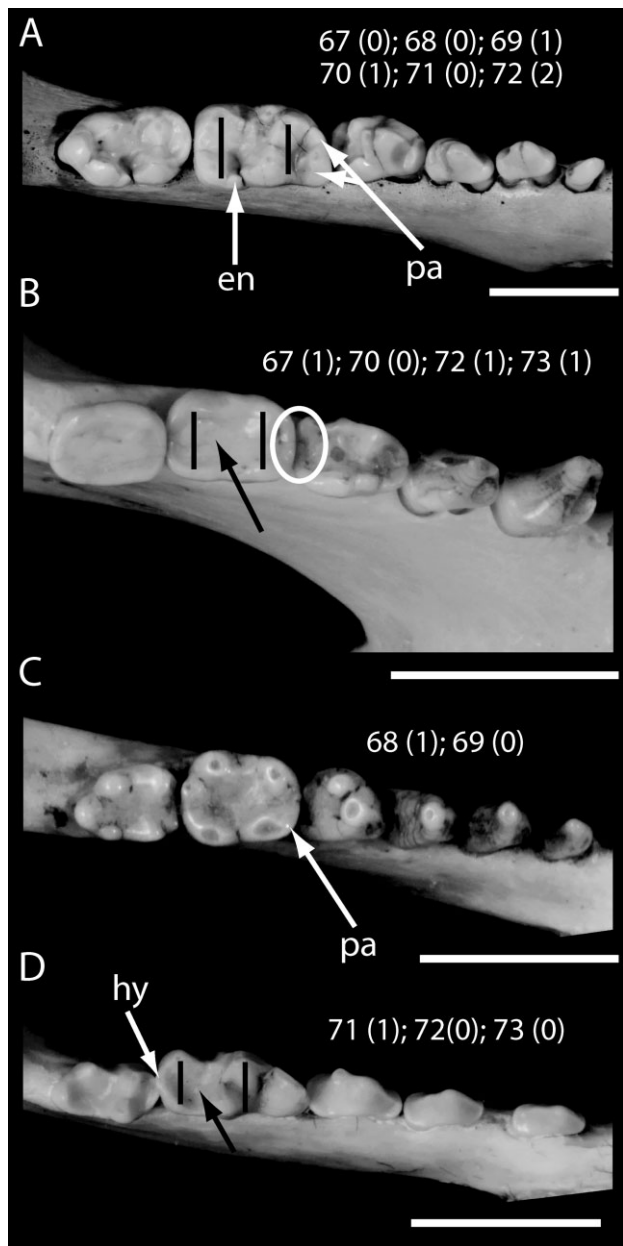


**Figure 33.** Characters 67, 68, 69, 70, 71, 72, and 73. Left dentition in dorsal view, anterior to the right. A, *Procyon lotor* TMM 778; B, *Potos flavus* MVZ 132125; C, *Bassaricyon alleni* FMNH 41502; D, *Bassariscus astutus* MVZ 192085. en, entoconulid; hy, hypoconulid; pa, paraconid; white circle: absence of paraconid; black lines: talonid versus trigonid width; black arrow: basined versus unbasined talonid. Scale bars = 1 cm.

68. m1 paraconid, size: (0) large; (1) small, Figure 33 (modified from Baskin, 2004: character 31).

The paraconid on the first lower molar is either large (state 0) or small (state 1). This character was originally incorporated with the previous character in

Baskin's (2004) analysis of procyonid relationships. Additionally, 'unreduced' and 'reduced' (Baskin, 2004) were exchanged for 'large' and 'small', respectively, because unreduced and reduced imply a priori assumptions about the evolution of the character.

**Distribution and polarity:** State (0) is the ancestral condition for Procyonidae. State (1) is derived only in *Bassaricyon alleni*.

69. m1 paraconid: (0) single cusped; (1) bifid, Figure 33 (modified from Baskin, 2004: character 30).

The m1 paraconid may also exhibit different morphologies in addition to size. The paraconid can either be single cusped (state 0) or bifid (state 1). The state 'with internal ridge to metaconid' was removed, because no taxon exhibited that condition.

**Distribution and polarity:** State (0) is plesiomorphic for Procyonidae. State (1) is derived in *Procyon lotor* and at node 12.

70. m1 entoconulid: (0) absent; (1) present, Figure 33 (Baskin, 2004: character 33).

The entoconulid on the first lower molar is either absent (state 0) or present (state 1). The character and character states were retained from Baskin (2004). However, the entoconulid was observed in *Procyon lotor* as a small cusp connected to the entoconid by a crest, and thus rescored accordingly.

**Distribution and polarity:** State (0) is derived at node 4. State (1) is present in *Urocyon cinereoargenteus*, *Mydaus javanensis*, and *Procyon lotor*. Thus the absence of the entoconulid is an autapomorphy of *Procyon lotor* within Procyonidae.

71. m1 hypoconulid: (0) absent; (1) present, Figure 33 (Baskin, 2004: character 34).

The hypoconulid on the first lower molar is either absent (state 0) or present (state 1). The character and character states were retained from Baskin (2004).

**Distribution and polarity:** State (0) is the plesiomorphic condition for Procyonidae. State (1) is present in *Martes pennanti* and *Bassariscus astutus*. This character was previously considered an autapomorphy of *Bassariscus* (Baskin, 2004); however, the inclusion of *Martes pennanti* indicates that state (1) is a local autapomorphy within Procyonidae.

72. m1 talonid width: (0) narrower than trigonid; (1) equal to trigonid; (2) wider than trigonid, Figure 33 (Baskin, 2004: character 35).

The talonid of the first lower molar exhibits varying transverse widths amongst taxa and is either narrower than the trigonid (state 0), equal in width to the trigonid (state 1), or wider than the trigonid (state

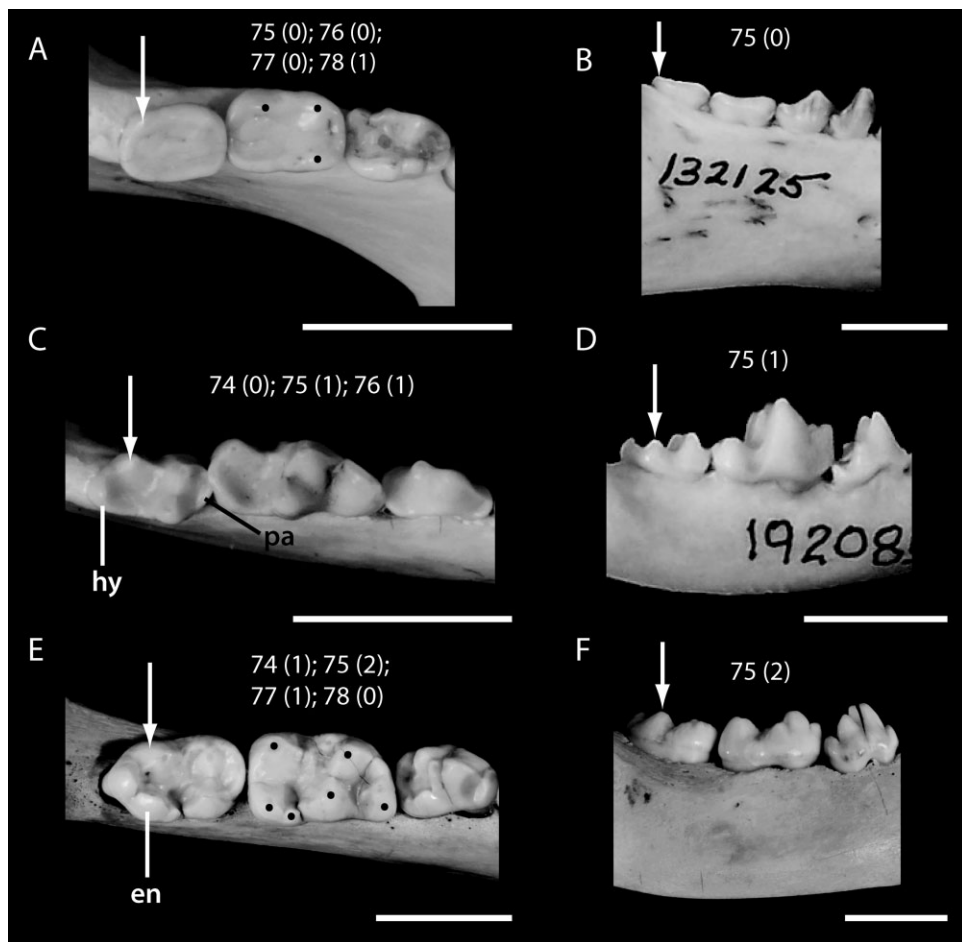


**Figure 34.** Characters 74, 75, 76, 77, and 78. A, C, E, left dentition in dorsal view; B, D, F, right dentition in lateral view anterior to the right. A, B, *Potos flavus* MVZ 132125; C, D, *Bassariscus astutus* MVZ 192085; E, F, *Procyon lotor* TMM 778. en, entoconulid; hy, hypoconulid; pa, paraconid; black dots: cusps; white arrow: hypoconid. Scale bars = 1 cm.

2). The character states were slightly modified from Baskin (2004) to include the reference point of 'trigond' in states (1) and (2) in addition to state (0).

Distribution and polarity: State (0) is reconstructed as the ancestral condition for Procyonidae. State (2) is derived at nodes 3 and 7. State (1) is derived only in *Potos flavus*, and thus an autapomorphy of this taxon.

73. m1 talonid: (0) basined; (1) unbasined, Figure 33 (Baskin, 2004: character 36).

The talonid of the first lower molar is either basined (state 0) or unbasined (state 1). The character and characters states were retained from Baskin (2004); however, *Bassaricyon alleni* was rescored as having a basined talonid.

Distribution and polarity: State (0) is the primitive condition for Procyonidae. State (1) is present only in *Potos flavus*.

74. m2 paraconid: (0) present; (1) absent, Figure 34 (Baskin, 2004: character 37).

The paraconid on the second lower molar is either present (state 0) or absent (state 1). The character and character states were retained from Baskin's (2004) analysis of procyonid relationships. I scored *Urocyon cinereoargenteus* as possessing a paraconid because younger specimens exhibit a very small cusp anteriorly along the cingulum, which is similar to the description of the paraconid in Baskin (2004).

Distribution and polarity: State (1) is the ancestral condition for Procyonidae. State (0) is present independently in *Urocyon cinereoargenteus* and *Bassariscus astutus*. Thus the presence of a paraconid is an autapomorphy of *Bassariscus astutus* within Procyonidae.

75. m2 hypoconid: (0) small; (1) enlarged; (2) larger than protoconid, Figure 34 (Baskin, 2004: character 38).

The size of the hypoconid on the second lower molar varies, from small (state 0) to enlarged and smaller than the protoconid (state 1) to larger than the protoconid (state 2). The character and character states were retained from Baskin (2004). However, *Potos flavus* was rescored as having a small hypoconid.

**Distribution and polarity:** State (1) is the plesiomorphic state for Procyonidae. State (0) is present independently in *Mydaus javanensis*, *Martes pennanti*, and *Potos flavus*. State (2) is derived at node 10 and a synapomorphy of the clade.

76. m2 hypoconulid: (0) absent; (1) present, Figure 34.

The hypoconulid on the second lower molar is either absent (state 0) or present (state 1).

**Distribution and polarity:** State (0) is the primitive condition, with state (0) derived at node 5, Procyonidae. The hypoconulid is secondarily lost in *Potos flavus*.

77. m2 entoconid: (0) absent; (1) present, Figure 34 (Decker & Wozencraft, 1991; modified from Baskin, 2004: character 40).

The entoconid of the second lower molar is either absent (state 0) or present (state 1). The character state ‘fused with reduced hypoconulid’ was removed from Baskin’s (2004) character because the entoconid and hypoconulid are always distinct and separate cusps in the genus *Nasua*, which was the only taxon scored as having that condition.

**Distribution and polarity:** State (0) is the ancestral condition for Procyonidae. State (1) is derived in *Bassaricyon alleni* and at node 10.

78. Number of cusps on molars: (0) greater than three; (1) fewer than or equal to three, Figure 34 (modified from Decker & Wozencraft, 1991).

The molars, both upper and lower, either have more than three cusps (state 0) or three or fewer cusps (state 1). The character was modified from Decker & Wozencraft (1991), to indicate that *Potos flavus* has three cusps on the lower molars. *Ailurus fulgens* was scored based on the upper molars only.

**Distribution and polarity:** State (0) is plesiomorphic for Procyonidae. State (1) is the derived state only in *Potos flavus*, and thus an autapomorphy of the taxon.

#### ELIMINATED CHARACTERS

Not all characters included in previous analyses (Decker & Wozencraft, 1991; Baskin, 2004) were incorporated in this analysis. Several characters were eliminated because they were uniform in all taxa sampled. These include the relative size of the foramen rotundum and the position of the internal

auditory meatus (Decker & Wozencraft, 1991), both of which were examined using HRXCT. Additional characters were excluded on the basis of intraspecific variation, such as presence and size of a supraorbital process (Decker & Wozencraft, 1991). I also excluded characters that I could not assess based on the specimens I sampled, including the shape of the malleus (Decker & Wozencraft, 1991). Characters with ambiguous character states, which I could not score, such as the shape of the protocone on the fourth upper premolar (Baskin, 2004: character 13), were also excluded.

#### PHYLOGENETIC RESULTS

The primary analysis, which includes all extant taxa plus the extinct *Edaphocyon pointblankensis*, yielded one MPT, 170 steps in length with a CI of 0.553, RI of 0.606, and RC of 0.335 (Fig. 35). Twelve characters are parsimony uninformative. The outgroup is rooted with *Urocyon cinereoargenteus*, with the mephitids (*Mydaus javanensis* plus *Conepatus leuconotus*) forming a clade separate from the mustelid (*Martes pennanti*). *Martes pennanti* is the sister taxon to Procyonidae, which is defined as the most recent common ancestor of *Bassariscus astutus*, *Potos flavus*, and *Procyon lotor* and all of that ancestor’s descendants, which here includes *Ailurus fulgens*.

Relationships within Procyonidae differ from both previous morphological and molecular analyses. *Bassariscus* is the most basal taxon, sister to a clade containing *Edaphocyon pointblankensis* plus all other procyonids and *Ailurus fulgens* (node 5, Fig. 35). *Edaphocyon pointblankensis*, the only included fossil taxon, is recovered within the crown. The remaining members of Procyonidae form two clades, one including *Ailurus*, *Bassaricyon*, and *Potos* and the other including *Procyon*, *Nasuella*, and *Nasua* spp. The red panda, *Ailurus fulgens*, is nested within crown Procyonidae and is the sister taxon to *Bassaricyon* plus *Potos*. The [*Bassaricyon* plus *Potos*] clade was recovered in both previous morphological phylogenies (Decker & Wozencraft, 1991; Baskin, 2004). *Procyon* is recovered outside of the clade containing the coati-mundis, *Nasuella* and *Nasua*, with both species of *Nasua* recovered as each other’s closest relative. The [*Procyon*, *Nasuella*, and *Nasua*] clade was recovered by Decker & Wozencraft (1991); a clade including *Procyon* plus *Nasua* was recovered by Baskin (2004), but *Nasuella* was not included in the analysis. Bremer decay support indices are highest (greater than or equal to three) for the following procyonid clades: [*Bassaricyon* plus *Potos*], [*Procyon*, *Nasuella*, and *Nasua*], and [*Nasuella* plus *Nasua*]. Bremer decay support indices with a value of one unite the following clades: [*Ailurus*, *Bassaricyon*, and *Potos*] and [*Nasua nasua* plus *Nasua narica*].

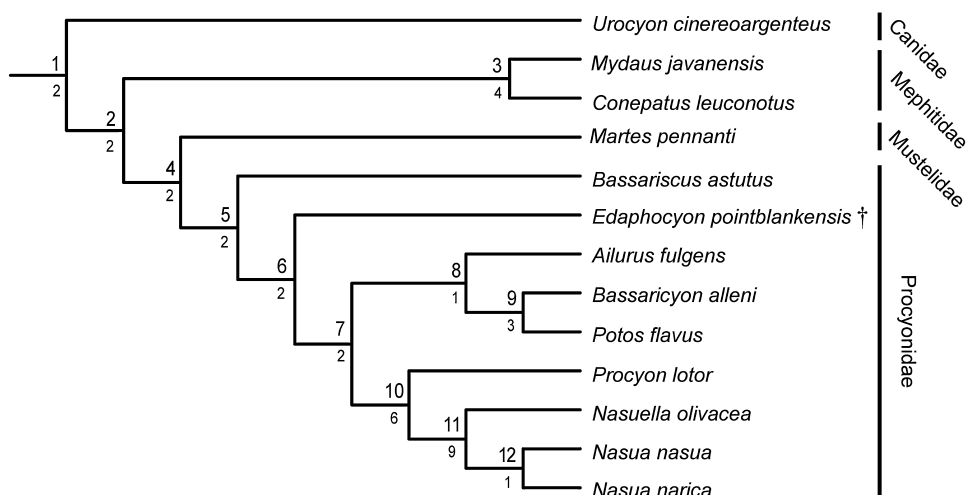


**Figure 35.** Most parsimonious tree recovered from the primary analysis. Numbers above the node indicate node number; numbers below the node indicate Bremer support value. †, extinct taxa.

An exhaustive search of only extant taxa yielded five MPTs, each 166 steps in length with a CI of 0.554, RI of 0.606, and RC of 0.336. Thirteen characters are parsimony uninformative. A strict consensus tree was computed for the five MPTs (Fig. 36A). The consensus tree recovers a polytomy including *Martes pennanti*, the mephitids, *Ailurus fulgens*, *Bassariscus astutus*, a clade containing *Bassaricyon allenii* and *Potos flavus*, and a clade containing *Procyon lotor*, *Nasuella olivacea*, *Nasua nasua*, and *Nasua narica*.

A heuristic search of all taxa that were at least 50 per cent complete relative to all considered characters, including all extant taxa plus *Edaphocyon pointblankensis* and *Probassariscus matthewi*, yielded one MPT. The consensus tree is 174 steps in length with a CI of 0.540, RI of 0.615, and RC of 0.332 (Fig. 36B). Twelve characters are parsimony uninformative. Ingroup relationships of this analysis are similar to those of the primary analysis. *Bassariscus astutus* remains the most basal member of Procyonidae, with *Probassariscus matthewi* nested within the crown and the sister taxon to the rest of Procyonidae. The rest of the topology is congruent with the primary analysis, with node A7 (Fig. 36B) congruent with node 6 (Fig. 35) of the primary analysis.

A heuristic search of all taxa that were at least 25 per cent complete relative to all considered characters, including all extant taxa plus *Edaphocyon pointblankensis*, *Probassariscus matthewi*, *Arctonasua gracilis*, and *Paranasua biradica*, yielded 11 MPTs. Each tree is 184 steps in length with a CI of 0.511, RI of 0.595, and RC of 0.304. Eleven characters are parsimony uninformative. A strict consensus tree was computed for the 11 MPTs (Fig. 36C) and recovers an

unresolved tritomy amongst the mephitids, mustelids, and procyonids. *Bassariscus astutus* and *Probassariscus matthewi* are recovered as basal members of Procyonidae, with *Probassariscus matthewi* as the sister taxon to the rest of Procyonidae. Within Procyonidae, at node B6, is a large polytomy that includes *Ailurus fulgens*, *Paranasua biradica*, *Arctonasua gracilis*, *Edaphocyon pointblankensis*, a clade containing *Bassaricyon allenii* and *Potos flavus*, *Procyon lotor*, and a clade containing *Nasuella olivacea*, *Nasua nasua*, and *Nasua narica*. Nodes B7 and B8 (Fig. 36C) are congruent with nodes 9 and 11 (Fig. 35), respectively, of the primary analysis.

The final taxon addition-deletion run included a heuristic search of all taxa, and yielded 342 MPTs, each 188 steps in length with a CI of 0.500, RI of 0.603, and RC of 0.302. A strict consensus tree was computed for the 342 MPTs (Fig. 36D), and recovers *Bassariscus astutus* as the sister taxon to a polytomy containing all other procyonids, with only the [*Procyon*, *Nasuella*, and *Nasua*] clade resolved. Node C7 (Fig. 36D) is congruent with node 10 (Fig. 35) of the primary analysis.

Two constraint trees were applied to the morphological analysis in order to assess effects of changing the controversial position of *Ailurus fulgens*. One constraint tree is based on the outgroup topology recovered by molecular analyses, and includes a canid as the most basal member of the outgroup, followed by the mephitids, *Ailurus fulgens*, and then *Martes pennanti*, the mustelid, as the sister taxon to Procyonidae (Fulton & Strobeck, 2006; Sato *et al.*, 2009; Eizirik *et al.*, 2010). The tree length increases by eight steps to 178, compared with the primary analysis, and has a CI of 0.517, RI of 0.554, and RC of 0.287. Another

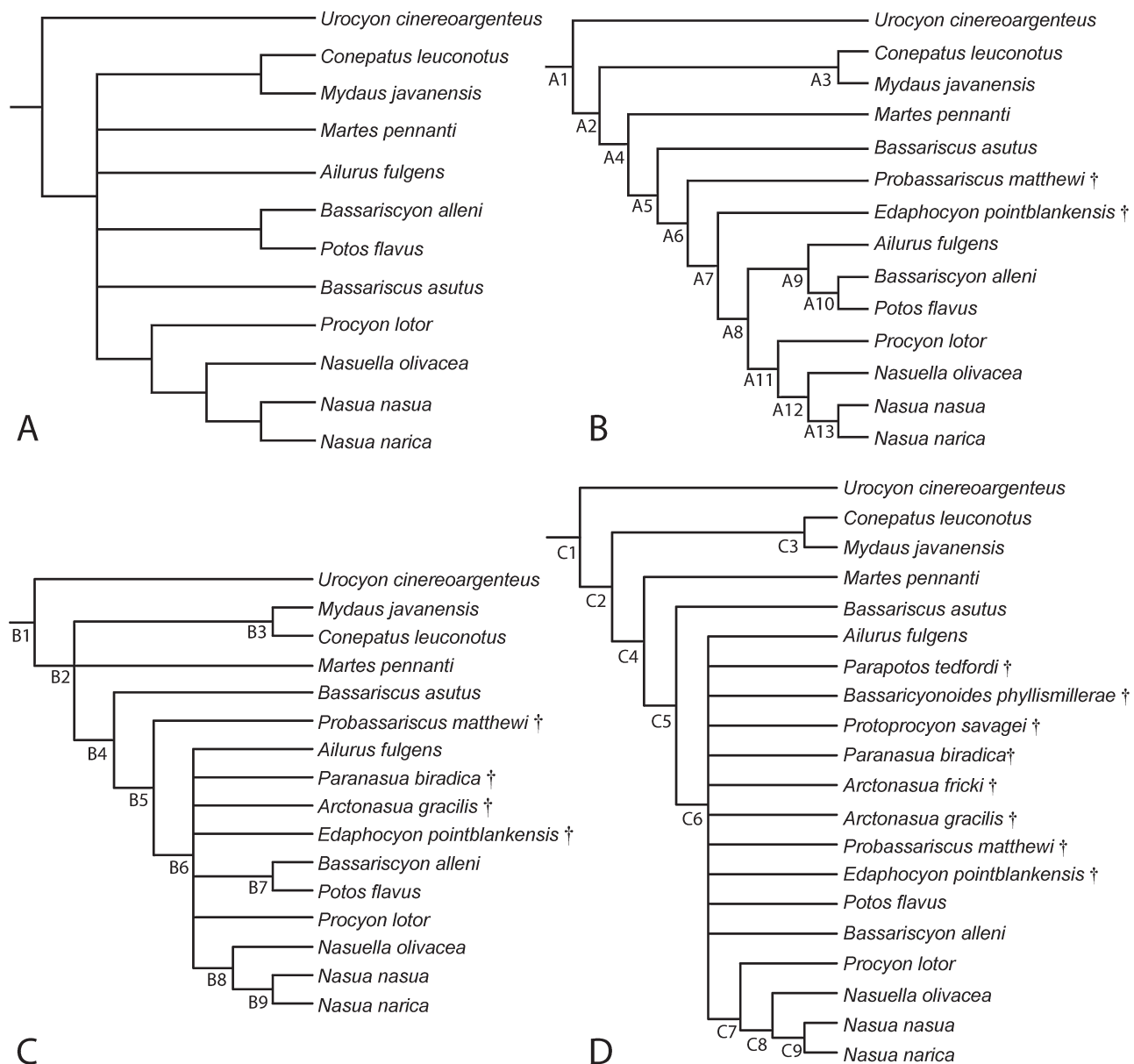


**Figure 36.** Strict consensus trees from the taxon addition–deletion runs. A, consensus tree of the five most parsimonious trees recovered by an exhaustive search of extant taxa only; B, most parsimonious tree recovered by a heuristic search of taxa with more than 50% of the characters scorable; C, consensus tree of the 11 most parsimonious trees recovered by a heuristic search of taxa with more than 25% of the characters scorable; D, consensus tree of the 342 most parsimonious trees recovered by a heuristic search of all taxa scored. Numbers below the nodes indicate node number. †, extinct taxa.

constraint tree was based on an outgroup topology rarely assessed in molecular analyses, although considered in Sato *et al.* (2009), which tested *Ailurus fulgens* as the sister taxon to Procyonidae. The tree length increases by seven steps to 177, and has a CI of 0.520, RI of 0.560, and RC of 0.291.

The morphological characters were mapped onto a molecular topology using MacClade 4 (Maddison & Maddison, 2005; Fig. 37A). The ingroup topology con-

sists of *Potos flavus* as the most basal member, with *Bassaricyon* and *Nasua* as sister taxa and *Procyon* and *Bassariscus* as sister taxa (Fulton & Strobeck, 2007; Koepfli *et al.*, 2007; Wolsan & Sato, 2010). The paraphyletic outgroup includes the canid as the most basal member, followed by the mephitids and *Ailurus fulgens*, with *Martes pennanti* as the sister taxon to Procyonidae (Fulton & Strobeck, 2006; Sato *et al.*, 2009; Eizirik *et al.*, 2010). The resulting tree is 193

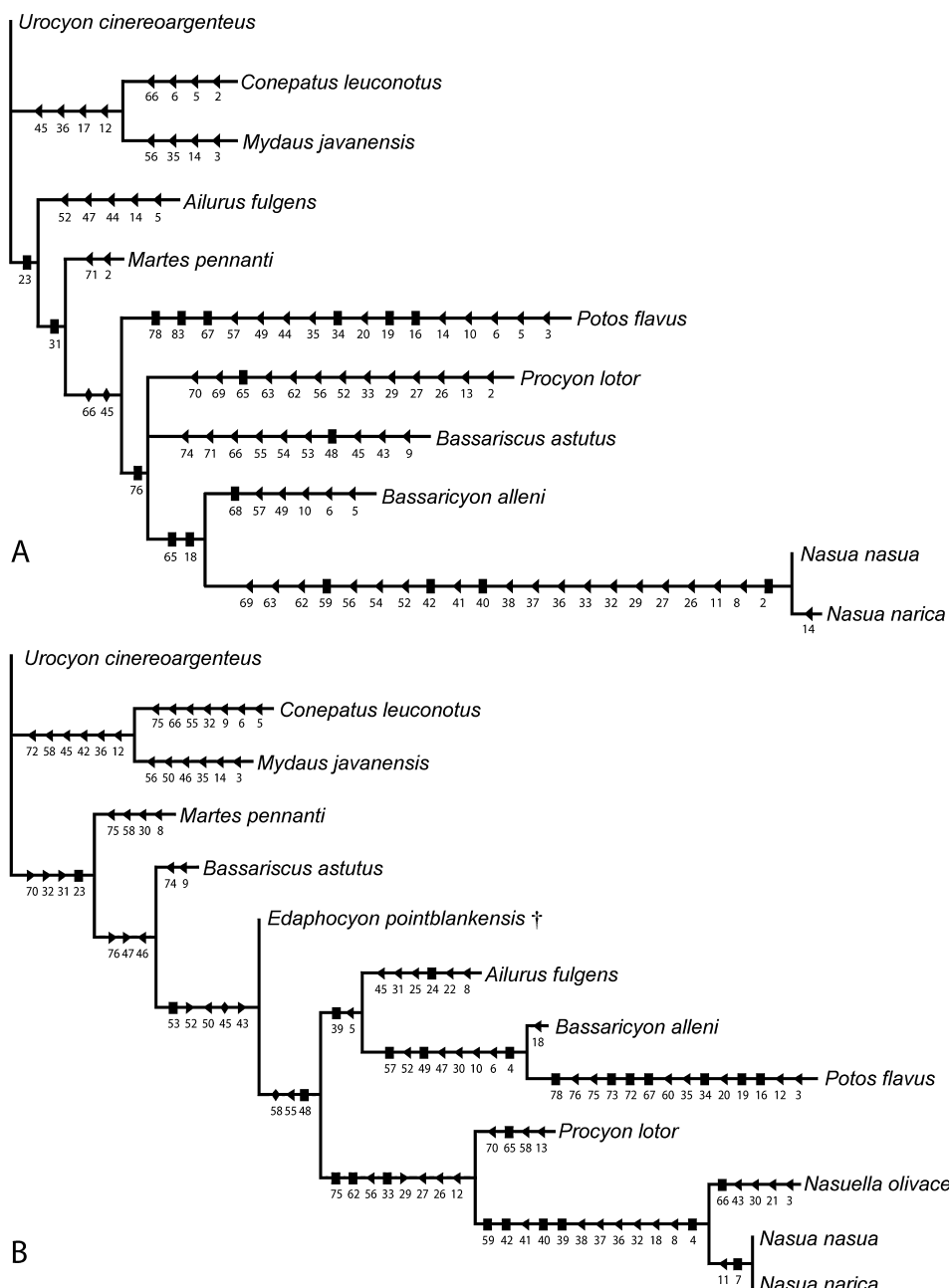


**Figure 37.** A, morphological characters optimized on the molecular topology, tree length equals 193 (modified from Fulton & Strobeck, 2007; Koepfli *et al.*, 2007; Eizirik *et al.*, 2010; Wolsan & Sato, 2010). B, morphological characters optimized on the morphological topology (primary analysis), tree length equals 170. Rectangle: character with a consistency index of 1; triangle with apex left: character is homoplastic outside the clade; triangle with apex right: character changes within the clade; diamond: character changes within and outside the clade. †, extinct taxa.

steps in length, with a CI of 0.477, RI of 0.369, and RC of 0.176.

#### CHARACTER EVOLUTION

The transformation of craniodental characters within Procyonidae was mapped onto the morphological

topology using MacClade 4 (Maddison & Maddison, 2005) and is shown in Figure 37B. Characters unambiguously optimized at node 5 Procyonidae, are P4 internal shelf present (46), P4 hypocone present (47), and m<sub>2</sub> hypoconulid present (76). Characters unambiguously optimized for node 6 are P<sub>3/p2-3</sub> either anteroposteriorly compressed or transversely broad-

ened (43), P4 protocone directly medial to the paracone (45), P4 metacone blade size reduced (50), P4 parastyle enlarged (52), and carnassial shear nonsectorial (53; CI of 1.0). Characters unambiguously optimized for node 7 are P4 hypocone large (48; CI of 1.0), upper molars rounded with reduced cusps (55), and M1 hypocone greatly reduced to absent (58). Characters unambiguously optimized for node 8 are ventral border of the infraorbital canal posterior to the dorsal border (5) and narrow grooves on the canine (39; CI of 1.0). Characters unambiguously optimized for node 9 are lateral profile of nasal straight (4; CI of 1.0), nasolabialis fossa absent (6), orbital wall of palatine diverging, not inflated (10), mastoid process horizontal in lateral view (30), P4 hypocone absent (47), P4 metacone blade absent (49; CI of 1.0), P4 parastyle small (52), and M1 parastyle small (57; CI of 1.0). Characters unambiguously optimized for node 10 are bony palate slightly concave (12), deep fossa for the tensor tympani, roofed by bony plate (26), floccular fossa absent or shallow (27), mastoid process extends ventral to the ventral margin of the meatal tube (29), angular process lies above the level of the tooth row (33; CI of 1.0), external cingulum of the upper molars reduced to absent (56), M1 metaconule posterior to the protocone (62; CI of 1.0), and m2 hypoconid is larger than protoconid (75; CI of 1.0). Characters unambiguously optimized for node 11 are nasal upturned anteriorly in lateral profile (4; CI of 1.0), deep antorbital fossa (8), rostral process of lacrimal present (18), elongate rostrum (32), I3 nearly equal in size to I1 and I2 (36), lower incisors procumbent (37), diastema between I2 and I3 present (38), broad grooves on the canine (39; CI of 1.0), upper canines flared laterally (40; CI of 1.0), diastema between C and P1/P2 present (41), P1 and p1 are double rooted (42; CI of 1.0), and M1 hypocone/internal cingulum posterior to the protocone (59; CI of 1.0). Characters unambiguously optimized for node 12 are a deep nasolabialis fossa (7; CI of 1.0) and deep zygomaticus muscular fossa in the orbital wall present (11).

## DISCUSSION

### APOMORPHIES OF PROCYONIDAE

Neither previous morphological analysis attempted to identify features that distinguish procyonids from other carnivorans (Decker & Wozencraft, 1991; Baskin, 2004). However, three possible apomorphies were suggested as diagnostic features of Procyonidae, including the presence of a squamosal epitympanic sinus, posterior orientation of the suprameatal fossa, and a distinctly bilobed baculum (Decker & Wozencraft, 1991). The use of HRXCT to investigate internal anatomy has revealed that the epitympanic

sinus is also present in *Urocyon cinereoargenteus* and *Martes pennanti*, and thus is not an unambiguous synapomorphy of Procyonidae. As I did not include postcranial material, I cannot assess the validity of a bilobed baculum as an apomorphy of Procyonidae.

The suprameatal fossa was suggested as a distinctive characteristic of Procyonidae in many previous works (including Segall, 1943; Hough, 1948; Hunt, 1974; Tedford, 1976). However, Decker & Wozencraft (1991) identified the posterior orientation of the fossa as the important distinguishing feature of Procyonidae, whereas Schmidt-Kittler (1981) and Wolsan (1993) identified the dorsally expanded roof as the distinguishing feature. Here, the suprameatal fossa (24) is not optimized as a synapomorphy of Procyonidae because *Ailurus fulgens* is recovered within crown Procyonidae. The position of *Ailurus fulgens* requires a reversal from the typical procyonid condition to the primitive musteloid condition of a shallow suprameatal fossa (Schmidt-Kittler, 1981).

Procyonidae is diagnosed (node 5, Fig. 35) by three synapomorphies in this analysis, including presence of an internal shelf on P4 (46), presence of a hypocone on P4 (46), and a hypoconulid present on m2 (76). The clade is not defined by any characters with a CI of 1.0; one character is also present in one outgroup and two are lost within the ingroup.

The presence of an internal shelf on P4 was identified as an apomorphy of Procyoninae, which includes *Broiliiana* plus New World procyonids (Baskin, 2004). When excluding Old World procyonids, the internal shelf is recovered as a synapomorphy of Procyonidae. The presence of the hypocone on P4 was previously used to unite Procyonidae (Mivart, 1885), but the loss of the hypocone in the Potosinae (*sensu* Decker & Wozencraft, 1991) and its absence in early *Bassariscus* spp. (Baskin, 2004) suggest that the presence of the hypocone is relatively plastic and is not an ideal diagnostic character. Previously, a posteroexternal hypoconulid was considered primitive for procyonids (Baskin, 2004). Here, the presence of a hypoconulid on m2 also unites Procyonidae, which is secondarily lost in *Potos flavus*. The loss of the m2 hypoconulid in *Potos flavus* represents one of many dental autapomorphies of the kinkajou within Procyonidae.

Our limited understanding of the relationships within Musteloidea based on morphology warrants more focused studies on the evolutionary relationships of groups within Musteloidea and the evolution of morphological characters within those clades. Further investigation of the character evolution in procyonids, mephitids, mustelids, and *Ailurus fulgens* may help identify the ancestral morphological

condition in each of these groups, and synapomorphies of these different groups.

#### CHARACTER EVOLUTION

Based on morphology, *Bassariscus astutus* is the least derived member of Procyonidae. The plesiomorphic morphology of *Bassariscus* was previously noted (Decker & Wozencraft, 1991). However, the taxon was recovered as the most basal member of Procyoninae (*sensu* Decker & Wozencraft, 1991), rather than at the base of Procyonidae. Most noticeably, the ringtail retains dentition adapted for a mesocarnivorous diet, also noted by Baskin (2004), with slender premolars (43), the protocone anteromedial to the paracone on P4 (45), an elongate metacone blade on P4 (50), sectorial carnassial shear (53), and triangular molars with distinct cusps (54).

*Edaphocyon pointblankensis* is more derived than *Bassariscus astutus*, as in previous analyses (Baskin, 2004), particularly with respect to dental morphology. The premolars are anteroposteriorly compressed or transversely broadened (43), the P4 protocone is directly medial to the paracone (45), and the metacone blade (50) and parastyle on P4 are reduced (52). However, the dentition still retains some features of a mesocarnivorous diet, such as triangular molars with distinct cusps (55) and a small hypocone on P4 (48). The ancestral condition at node 6 cannot be reconstructed owing to missing data for eight characters, four of which pertain to the morphology of the lower carnassial (m1). Characters that mark shifts in overall dental morphology and likely diet, such as the morphology of the m1 trigonid and respective height of the m1 protoconid, are equivocally optimized for *Edaphocyon pointblankensis*.

All other procyonids are united by three unambiguous dental characters: a large hypocone on P4 (48; CI of 1.0), rounded upper molars with reduced cusps (55), and a greatly reduced or absent hypocone on M1 (58). These morphologies are associated with overall changes in the premolar and molar shape, in which the teeth are more square or rounded with a greater number of cusps on the fourth premolar and reduced cusps on the molars. This is congruent with the general trend along the back-bone of the tree, in which there is a general loss of features associated with a mesocarnivorous diet and movement towards dentition associated with a more hypocarnivorous diet. This trend was recognized previously as a result of other phylogenetic studies of Procyonidae (Baskin, 1982, 2004).

One clade within Procyonidae includes the least carnivorous taxa, the folivorous *Ailurus fulgens* and the frugivorous *Bassaricyon alleni* and *Potos flavus*. The clade is united by two unambiguous characters,

one orbital (shape of the infraorbital canal, 5) and one dental (canines with narrow grooves, 39, CI of 1.0). There also are several characters ambiguously optimized as ancestral for the clade, including the position of Steno's foramen (2), anterior attachment of the vomer to the palate (17), and metacone and metaconule on M1 not connected by a crest (63). Implications of the phylogenetic position of the red panda, *Ailurus fulgens*, are discussed below.

As in previous morphological analyses, *Bassaricyon* and *Potos* are recovered as sister taxa (Decker & Wozencraft, 1991; Baskin, 2004) and are united by eight unambiguous synapomorphies. Four of those characters are cranial, including a straight profile of the nasal (4), absence of the nasolabialis fossa (6), uninflated orbital wall (10), and a horizontal mastoid process (30); the dental characters include the absence of the hypocone (47) and metacone blade (49; CI of 1.0) on P4, a small parastyle on P4 (52), and a small parastyle on M1 (57; CI of 1.0). The loss of cusps and orbital characters were identified as features probably exhibiting adaptive convergence, and thus supporting an incorrect morphological phylogeny of Procyonidae (Fulton & Strobeck, 2007; Koepfli *et al.*, 2007). However, the other characters that unite this clade are derived from disparate topographical regions of the skull and are more difficult to hypothesize as being caused by adaptive convergence. Additionally, the functional significance and adaptive pressures associated with characters such as an uninflated orbital wall and a horizontal mastoid process are not particularly clear and make claims of adaptive convergence more difficult to assert. The possibility cannot be discounted that these characters and others are associated with a particular diet and habitat as result of a common ancestor adapted for those resources.

Node 10, which includes *Procyon lotor* plus *Nasuella olivacea* and both *Nasua* species, is also supported by eight unambiguous synapomorphies. Five of those characters are craniomandibular, including a slightly concave bony palate (12), roofed fossa for the tensor tympani (26), absence of the floccular fossa (27), mastoid process that extends ventral to the meatal tube (29), and angular process above the level of the tooth row (33; CI of 1.0). The other three synapomorphies are dental, including absence of the external cingulum on the upper molars (56), the M1 metaconule posterior to the protocone (62; CI of 1.0), and the m2 hypoconid larger than the protoconid (75; CI of 1.0). The highly tuberculate molars (greater number of cusps) and long rostra were previously identified as evidence of ecological similarities and adaptive convergence (Koepfli *et al.*, 2007); however, in my analysis *Procyon lotor* is scored as having a rostrum of intermediate length (plesiomorphic for

*Procyonidae*, 32) and *Nasuella olivacea* and *Nasua* spp. are scored as having a relatively elongate rostrum. Although there is a general trend throughout the clade for more tuberculate molars, characters directly related to the addition of cusps cannot be unambiguously optimized as synapomorphies for node 10.

Node 11, which includes *Nasuella olivacea* and *Nasua* spp., is highly supported by 12 unambiguous synapomorphies. Four of the synapomorphies are rostral: nasals that are upturned anteriorly in lateral profile (4; CI of 1.0), a deep antorbital fossa (8), presence of the rostral process of the lacrimal (18), and an elongate rostrum (32). The remaining eight synapomorphies are dental, consisting of upper incisors of equal in size (36), procumbent lower incisors (37), presence of a diastema between I<sub>2</sub> and I<sub>3</sub> (38), broad canine grooves (39; CI of 1.0), upper canines flared laterally (40; CI of 1.0), presence of a diastema between C and P<sub>1</sub> (41), double rooted P<sub>1</sub> and p<sub>1</sub> (42; CI of 1.0), and M<sub>1</sub> internal cingulum posterior to protocone (59; CI of 1.0). The majority of the unique characters derived in the coatiundis relate to the rostral morphology and anterior dental characters. Several of these characters are thought to be correlated with function and behaviour, including rhinarial mobility, grooming, and insectivory (Decker & Wozenecraft, 1991). The two species of *Nasua* are united by two unambiguous synapomorphies, consisting of a deep nasolabialis fossa (7; CI of 1.0) and presence of a deep zygomaticus muscular fossa (11). The coatiundis are certainly recognizable and unique amongst procyonids in their derived rostral morphologies.

#### AFFINITIES OF THE RED PANDA

In this analysis, *Ailurus fulgens* is deeply nested within Procyonidae and shares several features only with members of Procyonidae, including anteroposteriorly compressed and transversely broadened premolars (43), a large hypocone (48) and enlarged parastyle (52) on P<sub>4</sub>, a prominent metaconule on M<sub>1</sub> (61), and narrow canine grooves (39). There are also several characters that *Ailurus fulgens* shares only with outgroup taxa, such as the presence of the alisphenoid canal (22), absence of the epitympanic sinus (25), reduced entotympanic inflation (28), and a rectangular paroccipital process (31). It is likely that long-branch attraction causes *Ailurus fulgens* to be recovered within Procyonidae. However, the deeply nested position of the red panda within the clade, as opposed to a more basal position, suggests either a close phylogenetic relationship or strong adaptive convergence towards herbivory, particularly with *Bassaricyon alleni* and *Potos flavus*.

Several recent molecular analyses have recovered *Ailurus fulgens* as sister to a [Procyonidae plus Mustelidae] clade (Fulton & Strobeck, 2006; Sato *et al.*, 2009; Eizirik *et al.*, 2010). However, only Sato *et al.* (2009) explicitly tested an alternative hypothesis of *Ailurus fulgens* as the sister taxon to Procyonidae. In their analysis only *Procyon* spp. was used to test the relationship; neither *Potos flavus*, the basal-most procyonid in molecular analyses (Wolsan & Sato, 2010), nor any other procyonid was sampled for the analysis. I believe that more explicit tests of the alternative hypotheses are required before we can begin to claim that there is ‘compelling resolution of the red panda’s phylogenetic position’ (Sato *et al.*, 2009: 908), particularly because previous molecular results yielded conflicting hypotheses of the phylogenetic position of *Ailurus fulgens* (Flynn *et al.*, 2000; Fulton & Strobeck, 2006). I applied two constraint trees to the morphological data to test alternative hypotheses of the relationships of *Ailurus fulgens*. Constraining the tree with the molecular outgroup topology requires an additional eight steps and reduces the number of characters diagnosing Procyonidae to one (presence of a hypoconulid on m<sub>2</sub>). Constraining the tree such that *Ailurus fulgens* is the sister taxon of Procyonidae requires an additional seven steps; there are no unambiguous apomorphies that unite Procyonidae when the red panda is constrained as the clade’s sister taxon.

The inclusion of fossils may prove to be the best evidence for decisive resolution of the phylogenetic position of the red panda. Recent North American cranial and postcranial discoveries of the new ailurid *Pristinailurus bristoli* (Wallace & Wang, 2004; Wallace & Schubert, 2006) will present a relative wealth of character data representing a large gap in the cladogram, and thus are promising with respect to resolving that conflict. Additionally, the discovery of an exceptionally preserved North American ailurid reduces concerns over recovering the currently Asian *Ailurus fulgens* within the otherwise exclusively New World crown clade. As there is no longer a doubt as to whether extinct taxa more closely related to the red panda inhabited North America, reservations about a close relationship between *Ailurus fulgens* and Procyonidae based solely on biogeography are not valid.

#### INCLUSION OF FOSSILS

Fossils are important in phylogenetic analyses because they represent additional character data that may show unique character combinations and intermediate states. Character states present in fossils potentially break up long branches, change character optimizations and the direction of character evolution, as well as provide evidence for adaptive

convergence with the discovery of plesiomorphic taxa lacking those homoplastic characters (Gauthier, Kluge & Rowe, 1988; Donoghue *et al.*, 1989). Furthermore, by excluding extinct taxa, the full diversity of the clade will never be represented. Although fossils may be missing large amounts of character data, they can still be informative if they possess unique character combinations or plesiomorphic states not present in extant taxa (Donoghue *et al.*, 1989).

When scored as composite taxa in previous analyses, fossil taxa may have produced misleading results (Wiens, 1998; Prendini, 2001; Brusatte, 2010). Accordingly, the species-exemplar approach is utilized for this analysis, which can decrease apparent phylogenetic resolution because of specimen completeness. When fossils with more than 50% of the data present are included (*Edaphocyon pointblankensis* and *Probassariscus matthewi*), ingroup relationships within Procyonidae are fully resolved; *Bassariscus astutus* is still recovered as the most basal member, and *Probassariscus matthewi* is more basal than *Edaphocyon pointblankensis*. Unambiguous synapomorphies at node A6 (Fig. 36B) are a vertical mastoid process (30), reduced metacone blade on P4 (50), m1 talonid wider than the trigonid (72), and m2 entoconid present (77). Three of these synapomorphies were ambiguously optimized in the primary analysis (30, 72, and 77). Unambiguous synapomorphies for node A7 (Fig. 36B) are anteroposteriorly compressed and transversely broadened premolars (43), protocone of P4 directly medial to the paracone (45), enlarged parastyle on P4 (52), and a nonsectorial carnassial shear (53). Thus, *Probassariscus matthewi* possesses features representative of the transition from mesocarnivory to hypocarnivory with a reduced metacone blade on P4 (50) and a wide talonid (72), but not to the extent that is observed in *Edaphocyon pointblankensis*. All other ingroup relationships within Procyonidae are congruent with the primary analysis.

When all taxa with more than 25% of the data present are added (now including *Paranasua biradica* and *Arctonasua gracilis*) 11 MPTs are recovered and the positions of *Paranasua biradica*, *Arctonasua gracilis*, and *Edaphocyon pointblankensis* are unresolved. Additionally, *Ailurus fulgens* is no longer recovered as the sister taxon to *Bassaricyon alleni* plus *Potos flavus*. The overall morphological trends recovered in the primary analysis are retained in this analysis, with some loss of resolution in the middle of the tree. Nodes B7 and B8 are congruent with relationships recovered at nodes 9 and 11, respectively, in the primary analysis (Fig. 35), suggesting strong morphological support for these clades. Additionally, there are several extinct taxa recovered between *Procyon lotor* and *Bassariscus astutus* suggesting that the

molecular data, rather than the morphological data, may exhibit long-branch attraction.

When all fossils scored for morphological characters are included, phylogenetic resolution is almost entirely lost within the ingroup, with a large polytomy present at node C6 (Fig. 36D). Procyonidae, however, is still recovered. A clade consisting of *Procyon lotor*, *Nasuella olivacea*, and *Nasua* spp. is recovered as a monophyletic group. Missing data, particularly in *Parapotos tedfordi*, *Bassaricyonoides phyllismillerae*, *Protoprocyon savagei*, and *Arctonasua fricki* inhibited recovery of a well-resolved phylogeny within Procyonidae. Previous analyses circumvented this issue through scoring composite taxa (Baskin, 2004). However, methods for determining scoring of composite taxa are often absent from analyses in which the method is used (Brusatte, 2010). In the most comprehensive analysis of procyonid relationships (Baskin, 2004), the method for determining individual character scoring was not provided. Thus, it was not always clear whether the most common character state or the plesiomorphic state of the composite taxon was used for the phylogenetic analysis. The use of the species-exemplar approach provides transparency and allows for reproducibility of phylogenetic analyses, but diminishes the chance of recovering a fully resolved tree. Although the completeness of the fossil record of Procyonidae may not allow for the recovery of a resolved procyonid phylogeny, this is the first analysis to explicitly examine the effects of missing data on the procyonid relationships.

#### MOLECULAR TOPOLOGY, MORPHOLOGICAL CHARACTERS

The morphological characters were mapped onto the molecular topology using MacClade 4 (Maddison & Maddison, 2005); character transformations are shown in Figure 37A. There are two unambiguous synapomorphies uniting a monophyletic Procyonidae; neither has a CI of 1.0. Characters uniting Procyonidae are a P4 protocone directly medial to the paracone (45) and an m1 protoconid lower than p4 (66). Each of these apomorphies are homoplastic within and outside of Procyonidae, and both are lost in *Bassariscus astutus*. An additional two characters are found in all procyonids, but have ambiguous character optimizations because of their distribution amongst the outgroup; these characters are a deep, dorsally expanded suprameatal fossa (24) and a well-developed internal shelf on P4 (46). Accordingly, there is a lack of strong, unambiguous morphological characters uniting Procyonidae based on the molecular topology.

The clade that consists of extant procyonids excluding *Potos flavus* (Fig. 37A) is united by one unambigu-

ous synapomorphy, the presence of the m2 hypoconulid (75). The m2 hypoconulid is present in all fossils except *Edaphocyon pointblankensis*, which does not have any lower dentition preserved. Inclusion of relatively complete fossils in the morphological analysis strengthens the hypothesis that *Bassariscus astutus* is a more basal member of the procyonids than *Potos flavus*. However, if *Potos flavus* is indeed the most basal member, and all sampled fossils are within the crown, the presence of the m2 hypoconulid may unite the extant *Bassaricyon*, *Nasua*, *Bassariscus*, and *Procyon*. That there is only one unambiguous synapomorphy for this clade lends minimal support to the node.

There are no unambiguous synapomorphies that unite *Bassariscus* and *Procyon*. Thus, the morphological support uniting these genera as sister taxa is poor. However, the clade containing *Bassaricyon* plus *Nasua* is supported by two unambiguous synapomorphies, each with a CI of 1.0, including the presence of the rostral process of the lacrimal (18) and m1 trigonid with the paraconid and metaconid close together (65). Thus, there is support for uniting the genera *Bassaricyon* and *Nasua*. There is significantly less support in the morphological analysis, however, for that sister relationship than for either [*Bassaricyon* plus *Potos*] or [*Nasua* plus *Procyon*], with both being supported by eight unambiguous synapomorphies.

Weak support for the molecular topology based on craniodental morphology is predictable because the two topologies are incongruent. However, such minimal morphological support suggests that there is either rampant convergence in craniodental morphology amongst taxa united in the morphological phylogeny, or that molecular techniques still have yet to uncover the relationships of Procyonidae. Adaptive convergence is certainly plausible, but the extent of morphological change required to support the molecular phylogeny calls the validity of the molecular topology into question. Members of Procyonidae, which are strongly united by morphology, may be similar functionally and ecologically because they evolved from an ancestor that exhibited those same ecologies and functional attributes, as opposed to adaptive convergence.

## CONCLUSIONS

This comprehensive analysis yields different phylogenetic results regarding the ingroup relationships of Procyonidae from previous morphological and molecular studies. Notably, *Bassariscus* was recovered as the sister taxon to all other procyonids, and *Ailurus fulgens*, often thought to be outside of Procyonidae, was found nested within Procyonidae. The recent discovery of a mostly complete North American

ailurid, *Pristinailurus bristoli*, shows that ailurids inhabited a much larger geographical range in the past, including North America. Thus, biogeography alone is not justification for excluding *Ailurus fulgens* from an exclusively New World crown clade.

The quantity and quality of the fossil material of procyonids and ailurids is poor relative to other carnivorans. When fossils at least 25% complete relative to all considered characters were incorporated in the analyses, ingroup relationships were fairly resolved. However, when all fossil taxa were included, much of the resolution within Procyonidae was lost. Thus, the usefulness of fossil procyonids in phylogenetic analyses is limited based on their completeness.

Postcranial and soft-tissue data were not included in this morphological analysis and may provide additional support for, or alternative hypotheses to, the recovered phylogeny. Additionally, postcranial anatomy may not be subject to the same selective pressures as craniodental anatomy. Therefore, postcranial and soft-tissue characters might aid in resolving the conflict between the morphological and molecular hypotheses.

Although molecular systematists often invoke adaptive convergence as the most likely cause of morphological and molecular incongruence, the number of craniodental characters that would have to be convergent within Procyonidae is extraordinarily high. A combined analysis of morphological and molecular data may provide the best indication of the true topology, reveal relationships not recovered by either morphology or molecules alone, and better address issues of possible adaptive convergence within Procyonidae.

## ACKNOWLEDGEMENTS

I completed this project as part of my Master's thesis at the University of Texas at Austin. I thank my advisor Tim Rowe and committee members Chris Bell and Matt Colbert for their many suggestions and guidance. Additionally, I thank Ken Rose and Dave Weishampel, as well as fellow graduate students Bhart-Anjan Bhullar, Kerin Claeson, Katie Criswell, Eric Ekdale, Christian George, Jen Olori, and Michelle Stocker for their input and suggestions. I am grateful for the generous loans of specimens from the Field Museum of Natural History, Museum of Vertebrate Zoology, Royal Ontario Museum, and Vertebrate Paleontology Laboratory branch of the Texas Memorial Museum. Financial support from the Jackson School of Geosciences and Geology Foundation covered the costs of numerous HRXCT scans. I would also like to thank the staff of the High-Resolution X-ray Computed Tomography Facility (UTCT) for

scanning and initial image processing of the specimens. Finally, I wish to recognize Blaire Van Valkenburgh for additional loans of HRXCT scan data.

## REFERENCES

- Agnarsson I, Kuntner M, May-Colado LJ.** 2010. Dogs, cats, and kin: a molecular species-level phylogeny of Carnivora. *Molecular Phylogenetics and Evolution* **54**: 726–745.
- Ahrens H.** 2009. Novel insights on the basiscranium of *Buisnictis chisoensis* with implications for its phylogenetic position. *Journal of Vertebrate Paleontology* **29** (Suppl. 3): 52A.
- Baskin JA.** 1982. Tertiary Procyoninae (Mammalia: Carnivora) of North America. *Journal of Vertebrate Paleontology* **2**: 71–93.
- Baskin JA.** 1989. Comments on New World Tertiary Procyonidae (Mammalia: Carnivora). *Journal of Vertebrate Paleontology* **9**: 110–117.
- Baskin JA.** 2003. New procyonines from the Hemingfordian and Barstovian of the Gulf Coast and Nevada, including the first fossil record of the Potosini. In: Flynn LJ, ed. Vertebrate fossils and their context: contributions in honor of Richard H. Tedford. *Bulletin of the American Museum of Natural History* **278**: 125–146.
- Baskin JA.** 2004. *Bassariscus* and *Probassariscus* (Mammalia, Carnivora, Procyonidae) from the early Barstovian (middle Miocene). *Journal of Vertebrate Paleontology* **24**: 709–720.
- Bininda-Emonds OR, Gittleman JL, Purvis A.** 1999. Building large trees by combining phylogenetic information: a complete phylogeny of the extant Carnivora (Mammalia). *Biological Reviews* **74**: 143–175.
- Brusatte SL.** 2010. Representing supraspecific taxa in higher-level phylogenetic analyses: guidelines for palaeontologists. *Palaeontology* **53**: 1–9.
- Decker DM, Wozencraft WC.** 1991. Phylogenetic analysis of recent procyonid genera. *Journal of Mammalogy* **72**: 42–55.
- Donoghue MJ, Doyle JA, Gauthier J, Kluge AG, Rowe T.** 1989. The importance of fossils in phylogeny reconstruction. *Annual Review of Ecology and Systematics* **20**: 431–460.
- Dragoo JW, Honeycutt RL.** 1997. Systematics of mustelid-like carnivores. *Journal of Mammalogy* **78**: 426–443.
- Eizirik E, Murphy WJ, Koepfli KP, Johnson WE, Dragoo JW, Wayne RK, O'Brian SJ.** 2010. Pattern and timing of diversification of the mammalian order Carnivora inferred from multiple nuclear gene sequences. *Molecular Phylogenetics and Evolution* **56**: 49–60.
- Evans HE.** 1993. *Miller's anatomy of the dog*, 3rd edn. Philadelphia, PA: W.B. Saunders Company.
- Finarelli JA.** 2008. A total evidence phylogeny of the Arctoidea (Carnivora:Mammalia): relationships among basal taxa. *Journal of Mammalian Evolution* **15**: 231–259.
- Flower WH.** 1869. On the value of the characters of the base of the cranium in the classification of the Order Carnivora, and on the systematic position of *Bassaris* and other disputed forms. *Proceedings of the Zoological Society of London* **37**: 4–37.
- Flynn JJ, Finarelli JA, Zehr S, Hsu J, Nedbal MA.** 2005. Molecular phylogeny of the Carnivora (Mammalia): assessing the impact of increased sampling on resolving enigmatic relationships. *Systematic Biology* **54**: 317–337.
- Flynn JJ, Nedbal MA, Dragoo JW, Honeycutt RL.** 2000. Whence the red panda? *Molecular Phylogenetics and Evolution* **17**: 190–199.
- Fulton TL, Strobeck C.** 2006. Molecular phylogeny of the Arctoidea (Carnivora): effect of missing data on supertree and supermatrix analyses of multiple gene data sets. *Molecular Phylogenetics and Evolution* **41**: 165–181.
- Fulton TL, Strobeck C.** 2007. Novel phylogeny of the raccoon family (Procyonidae: Carnivora) based on nuclear and mitochondrial DNA evidence. *Molecular Phylogenetics and Evolution* **43**: 1171–1177.
- Gauthier J, Kluge AG, Rowe T.** 1988. Amniote phylogeny and the importance of fossils. *Cladistics* **4**: 105–209.
- Gehrt SD.** 2003. Raccoon (*Procyon lotor*) and allies. In: Feldhamer GA, Thompson BC, Chapman JA, eds. *Wild mammals of North America*, 2nd edn. Baltimore: Johns Hopkins University Press, 611–634.
- Gill T.** 1874. Arrangement of the families of mammals. *Smithsonian Miscellaneous Collections* **11**: 1–98.
- Goldman EA.** 1950. Raccoons of North and Middle America. *North American Fauna* **60**: 1–153.
- Gray JE.** 1869. *Catalogue of carnivorous, pachydermatous, and edentate Mammalia in the British Museum*. London: Taylor and Francis.
- Hawkins JA, Hughes CE, Scotland RW.** 1997. Primary homology assessment, characters and character states. *Cladistics* **13**: 275–283.
- Hollister N.** 1915. The genera and subgenera of raccoons and their allies. *Proceedings of the United States National Museum* **49**: 143–150.
- Hough JR.** 1948. The auditory region in some members of the Procyonidae, Canidae, and Ursidae. *Bulletin of the American Museum of Natural History* **92**: 67–118.
- Hunt RM.** 1974. The auditory bulla in Carnivora: an anatomical basis for reappraisal of carnivor evolution. *Journal of Morphology* **143**: 21–75.
- Kennedy ML, Lindsay SL.** 1984. Morphologic variation in the raccoon, *Procyon lotor*, and its relationship to genic and environmental variation. *Journal of Mammalogy* **65**: 195–205.
- Koepfli K-P, Gompper ME, Eizirik E, Ho C-C, Linden L, Maldonado JE, Wayne RK.** 2007. Phylogeny of the Procyonidae (Mammalia: Carnivora): molecules, morphology and the Great American Interchange. *Molecular Phylogenetics and Evolution* **43**: 1076–1095.
- Linares OJ.** 1982. Tres nuevos carnívoros procionidos fosiles del Mioceno de Norte y Sudamerica. *Ameghiniana* **18**: 113–121.
- Maddison DR, Maddison WP.** 2005. *MacClade 4: analysis of phylogeny and character evolution*. Version 4. Sunderland, MA: Sinauer Associates, Inc.
- Maddison WP, Donoghue MJ, Maddison DR.** 1984. Outgroup analysis and parsimony. *Systematic Zoology* **33**: 83–103.

- Mivart SG.** 1885. On the anatomy, classification and distribution of the Arctoidea. *Proceedings of the Zoological Society of London* **53**: 340–404.
- Pimentel RA, Riggins R.** 1987. The nature of cladistic data. *Cladistics* **3**: 201–209.
- Pocock RI.** 1921. The external characters and classification of the Procyonidae. *Proceedings of the Zoological Society of London* **91**: 389–422.
- Prange S, Gehrt SD, Wiggers EP.** 2003. Demographic factors contributing to high raccoon densities in urban landscapes. *The Journal of Wildlife Management* **67**: 324–333.
- Prendini L.** 2001. Species or supraspecific taxa as terminals in cladistic analysis? Groundplans versus exemplars revisited. *Systematic Biology* **50**: 290–300.
- Ritke ME.** 1990. Sexual dimorphism in the raccoon (*Procyon lotor*): morphological evidence for intrasexual selection. *American Midland Naturalist* **124**: 342–351.
- Sato JJ, Wolsan M, Minami S, Hosoda T, Sinaga MH, Hiyama K, Yamaguchi Y, Suzuki H.** 2009. Deciphering and dating the red panda's ancestry and early adaptive radiation of Musteloidea. *Molecular Phylogenetics and Evolution* **53**: 907–922.
- Schmidt-Kittler N.** 1981. Zur Stammesgeschichte der marder verwandten Raubtiergruppen (Musteloidea, Carnivora). *Eclogae Geologicae Helvetiae* **74**: 753–801.
- Segall W.** 1943. The auditory region of the arctoid carnivores. *Field Museum of Natural History, Zoological Series* **29**: 33–59.
- Slowinski JB.** 1993. 'Unordered' versus 'ordered' characters. *Systematic Biology* **42**: 155–165.
- Story HE.** 1951. The carotid arteries in the Procyonidae. *Fieldiana: Zoology* **32**: 479–557.
- Strong EE, Lipscomb D.** 1999. Character coding and inapplicable data. *Cladistics* **15**: 363–371.
- Swofford DL.** 2002. *PAUP\*: phylogenetic analysis using parsimony (\*and other methods)*, version 4. Sunderland, MA: Sinauer Associates, Inc.
- Tedford RH.** 1976. Relationship of pinnipeds to other carnivores (Mammalia). *Systematic Zoology* **25**: 363–374.
- Turner HN.** 1848. Observations relating to some of the foramina at the base of the skull in Mammalia, and on the classification of the order Carnivora. *Proceedings of the Zoological Society of London* **16**: 63–87.
- Wallace SC, Schubert BW.** 2006. Postcrania of Bristol's red panda, *Pristinailurus bristoli* from the Late Miocene of the southern Appalachians. *Journal of Vertebrate Paleontology* **26** (Suppl. 3): 136A.
- Wallace SC, Wang X.** 2004. Two new carnivorans from an unusual late Tertiary forest biota in eastern North America. *Nature* **431**: 556–559.
- Wang X.** 1997. New cranial material of *Simocyon* from China, and its implications for phylogenetic relationship to the red panda (*Ailurus*). *Journal of Vertebrate Paleontology* **17**: 184–198.
- Wang X, Tedford RH.** 1994. Basicranial anatomy and phylogeny of primitive canids and closely related miacids (Carnivora: Mammalia). *American Museum Novitates* **3092**: 1–34.
- Wiens JJ.** 1998. The accuracy of methods for coding and sampling higher-level taxa for phylogenetic analysis: a simulation study. *Systematic Biology* **47**: 397–413.
- Wolsan M.** 1993. Phylogeny and classification of early European Mustelida (Mammalia: Carnivora). *Acta Theriologica* **38**: 345–384.
- Wolsan M.** 1999. Oldest mephitine cranium and its implications for the origin of skunks. *Acta Palaeontologica Polonica* **44**: 223–230.
- Wolsan M, Sato JJ.** 2010. Effects of data incompleteness on the relative performance of parsimony and Bayesian approaches in a supermatrix phylogenetic reconstruction of Mustelidae and Procyonidae (Carnivora). *Cladistics* **26**: 168–194.
- Wozencraft WC.** 2005. Order Carnivora. In: Wilson DE, Reeder DM, eds. *Mammal species of the world: a taxonomic and geographic reference*, 3rd edn. Baltimore: Johns Hopkins University Press, 532–628.
- Wright T, Lundelius E.** 1963. Post-Pleistocene raccoons from Central Texas and their zoogeographic significance. *The Pearce-Sellards Series* **2**: 1–21.
- Wyss AR, Flynn JJ.** 1993. A phylogenetic analysis and definition of the Carnivora. In: Szalay FS, Novacek MJ, McKenna MC, eds. *Mammal phylogeny: placentals*. 2. New York: Springer-Verlag, 32–52.

**APPENDIX 1**  
Character matrix. Missing data indicated by (?), and inapplicable data indicated by (-)

|   | 1 | 2 | 3 |
|---|---|---|---|
|   | 0 | 0 | 0 |
| <i>Procyon lotor</i>                    | 1 | 2 | 0 |
| <i>Bassarisus astutus</i>               | 1 | 0 | 0 |
| <i>Nasua nasua</i>                      | 1 | 1 | 0 |
| <i>Nasua narica</i>                     | 1 | 1 | 0 |
| <i>Nosuella olivacea</i>                | 1 | 1 | 2 |
| <i>Bassaricyon aleni</i>                | 1 | 0 | 0 |
| <i>Potos flavus</i>                     | 1 | 0 | 1 |
| <i>Edaphocyon pointblankensis</i>       | ? | ? | ? |
| <i>Probassarisus matthewi</i>           | ? | ? | ? |
| <i>Arctonanus griseus</i>               | ? | ? | ? |
| <i>Arctonanus frickii</i>               | ? | ? | ? |
| <i>Paranasua biradica</i>               | ? | ? | ? |
| <i>Protoprocyon savagei</i>             | ? | ? | ? |
| <i>Bassaricyonoidea phyllismillerae</i> | ? | ? | ? |
| <i>Parapotos fedjordi</i>               | ? | ? | ? |
| <i>Ailurus fulgens</i>                  | 1 | 0 | 1 |
| <i>Urocyon cinereoargenteus</i>         | 0 | 0 | 1 |
| <i>Mydaus javanensis</i>                | 1 | 0 | 1 |
| <i>Conspatus leuconotus</i>             | 1 | 2 | 0 |
| <i>Martes pennanti</i>                  | 1 | 2 | ? |
|   | 4 | 5 | 6 |
|   | 0 | 0 | 0 |
| <i>Procyon lotor</i>                    |   |   | 7 |
| <i>Bassarisus astutus</i>               |   |   | 7 |
| <i>Nasua nasua</i>                      |   |   | 8 |
| <i>Nasua narica</i>                     |   |   |   |
| <i>Nosuella olivacea</i>                |   |   |   |
| <i>Bassaricyon aleni</i>                |   |   |   |
| <i>Potos flavus</i>                     |   |   |   |
| <i>Edaphocyon pointblankensis</i>       |   |   |   |
| <i>Probassarisus matthewi</i>           |   |   |   |
| <i>Arctonanus griseus</i>               |   |   |   |
| <i>Arctonanus frickii</i>               |   |   |   |
| <i>Paranasua biradica</i>               |   |   |   |
| <i>Protoprocyon savagei</i>             |   |   |   |
| <i>Bassaricyonoidea phyllismillerae</i> |   |   |   |
| <i>Parapotos fedjordi</i>               |   |   |   |
| <i>Ailurus fulgens</i>                  |   |   |   |
| <i>Urocyon cinereoargenteus</i>         |   |   |   |
| <i>Mydaus javanensis</i>                |   |   |   |
| <i>Conspatus leuconotus</i>             |   |   |   |
| <i>Martes pennanti</i>                  |   |   |   |

## APPENDIX 2

Specimens examined.

| Taxon                             | Institution | Specimen number  |
|-----------------------------------|-------------|--|
| <i>Procyon lotor</i>              | TMM         | 129, 360, 363, 392, 417, 778, 917, 1139, 1146, 1167, 2220, 2271, 3506,<br>3508, 3556, 3744, 3764, 3831, 3887, 4136 |
|                                   | LACM        | 52261  |
| <i>Bassariscus astutus</i>        | MVZ         | 91008, 97573, 192085   |
|                                   | TMM         | 473, 1036, 1059  |
| <i>Nasua nasua</i>                | FMNH        | 21400, 70728, 79872  |
| <i>Nasua narica</i>               | FMNH        | 14013, 14471, 51101  |
|                                   | TMM         | 491, 4162  |
| <i>Nasuella olivacea</i>          | FMNH        | 70745, 70746, 70749  |
| <i>Bassaricyon alleni</i>         | FMNH        | 41502, 62079, 65788  |
| <i>Potos flavus</i>               | MVZ         | 132125, 155212, 155216   |
|                                   | TMM         | 5558   |
| <i>Edaphocyon pointblankensis</i> | TMM         | 31190 -76  |
| <i>Ailurus fulgens</i>            | ROM         | 180  |
| <i>Urocyon cinereoargenteus</i>   | MVZ         | 86861, 114285; 218235; 218693  |
|                                   | TMM         | 553, 2063  |
| <i>Mydaus javanensis</i>          | FMNH        | 68729, 68731 ( <i>Mydaus marchei</i> 62878)  |
| <i>Conepatus leuconotus</i>       | TMM         | 3808   |
| <i>Martes pennanti</i>            | MVZ         | 23686, 29809, 31133, 186282  |

## APPENDIX 3

References for taxa scored from the literature, with specimens referred to each taxon in the description listed.

| Taxon                                   | Reference                   | Specimen numbers                               |
|---|-----------------------------|--|
| <i>Probassariscus matthewi</i>          | Linares, 1982               | F:AM 25370, 25371, 25372, 25373, 25374, 25375, |
|   | Baskin, 1989                | 49100, 49102, 49103                            |
|   | Baskin, 2004                |  |
| <i>Arctonasua gracilis</i>              | Baskin, 1982                | F:AM 105248                                    |
| <i>Arctonasua fricki</i>                | Baskin, 1982                | F:AM 49485, 50053, 50054                       |
| <i>Paranasua biradica</i>               | Baskin, 1982                | UF 22297, 24391-24401, 24829                   |
| <i>Protoprocyon savagei</i>             | Baskin, 1982; Linares, 1982 | F:AM 25210                                     |
| <i>Bassaricyonoidea phyllismillerae</i> | Baskin, 2003                | KUVP 130678                                    |
| <i>Parapotos tedfordi</i>               | Baskin, 2003                | F:AM 63289                                     |

## APPENDIX 4

High-resolution X-ray computed tomography scanning parameters.

| Taxon                           | Specimen number | Slice thickness (mm) | Interslice spacing (mm) | Field of reconstruction (mm) | Number of slices |
|---------------------------------|-----------------|----------------------|-------------------------|------------------------------|------------------|
| <i>Procyon lotor</i>            | TMM 778         | 0.1639               | 0.1639                  | 75                           | 701              |
|                                 | LACM 52261      | 0.1686               | 0.1686                  | 79                           | 724              |
| <i>Bassariscus astutus</i>      | TMM 473         | 0.09721              | 0.09721                 | 45                           | 786              |
| <i>Nasua nasua</i>              | FMNH 21400      | 0.1567               | 0.1567                  | 73                           | 809              |
| <i>Nasua narica</i>             | FMNH 14013      | 0.1428               | 0.1428                  | 66                           | 856              |
| <i>Nasuella olivacea</i>        | FMNH 70746      | 0.09755              | 0.09755                 | 44.5                         | 1040             |
| <i>Bassaricyon alleni</i>       | FMNH 41502      | 0.1185               | 0.1185                  | 55                           | 706              |
| <i>Potos flavus</i>             | USNM 291066     | 0.1615               | 0.1615                  | 72                           | 555              |
| <i>Ailurus fulgens</i>          | ROM 180         | 0.1707               | 0.1707                  | 79                           | 649              |
| <i>Urocyon cinereoargenteus</i> | UCLA 6928       | 0.241                | 0.241                   | 62                           | 477              |
| <i>Mydaus javanensis</i>        | FMNH 62878      | 0.09406              | 0.09406                 | 43                           | 877              |
| <i>Martes pennanti</i>          | MVZ 29809       | 0.1567               | 0.1567                  | 73                           | 801              |